AD-A124 759 DESIGN AND DEVELOPMENT OF A LASER WAVEMETER(U) AIR FORCE INST OF TECH WRIGHT-PATTERSON AFB OH SCHOOL OF ENGINEERING H W LADEWIG DEC 82 AFIT/GEO/PH/82D-7 1/1

UNCLASSIFIED F/G 20/5 NL

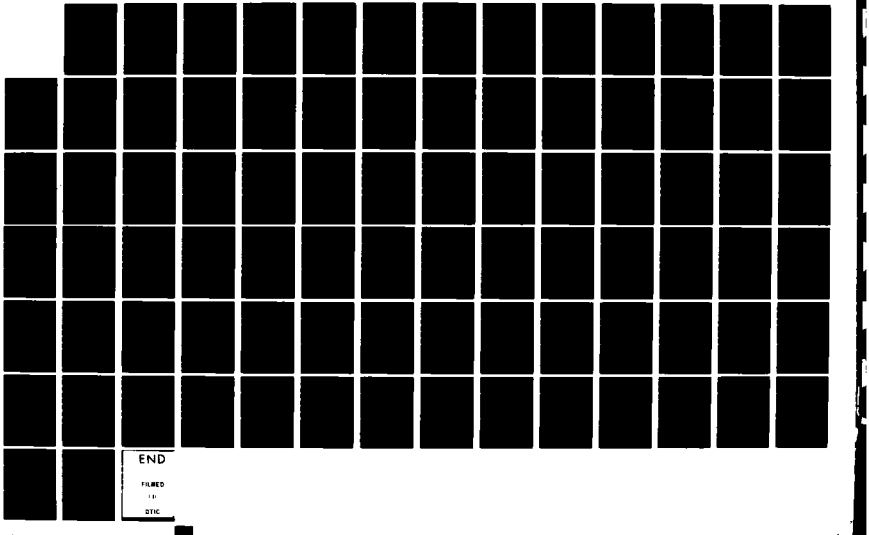

END

FILMED

DTIC

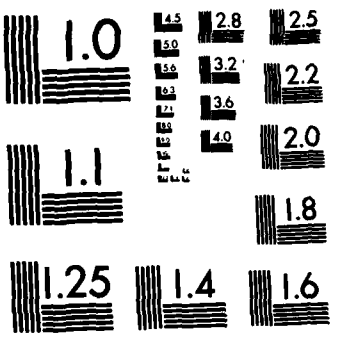

DESIGN AND DEVELOPMENT

OF A

LASER WAVEMETER

THESIS

AFIT/GEO/PH/82D-7 Harry W. Ladewig
Capt USAF

DEPARTMENT OF THE AIR FORCE
AIR UNIVERSITY (ATC)
AIR FORCE INSTITUTE OF TECHNOLOGY

Wright-Patterson Air Force Base, Ohio

AFIT/GEO/PH/82D-7

DESIGN AND DEVELOPMENT

OF A

LASER WAVEMETER

THESIS

AFIT/GEO/PH/82D-7 Harry W. Ladewig
Capt USAF

Approved for public release; distribution unlimited

AFIT/GEO/PH/82D-7

DESIGN AND DEVELOPMENT OF A LASER WAVEMETER

THESIS

Presented to the Faculty of the School of Engineering
of the Air Force Institute of Technology
Air University
in Partial Fulfillment of the
Requirements for the Degree of
Master of Science

by
Harry W. Ladewig, B.S.
Capt USAF
Graduate Electro-Optics
December 1982

Preface

Although the end result of this thesis project was not a working wavemeter, it was definitely a valuable learning experience. I have tried to document the project well enough that it can be continued with a minimum of wasted effort in attempts to figure out what something is supposed to do.

I owe a debt of gratitude to all of the craftsmen of the AFIT Model Fabrication Division, particularly to Russell Murray for the excellent job he did on the air rail and to John Brohas for his work on other components and general guidance. I also want to thank the Physics Department lab technicians, Ron Gabriel and George Gergal, for their help and advice.

Without the timely advice and encouragement provided by my advisor, Dr. W.B. Roh, I probably would not have gotten this wavemeter as far along towards completion as I did. For this, I thank him.

My wife, Carla, deserves special recognition for her support and prayers throughout this project and for all of the effort she expended converting my hieroglyphics into this polished final report.

Above all, I owe thanks to God. Without His guidance, both to me and to those who helped me, none of this would have been possible.

Contents

List of Figures

Abstract

The purpose of this thesis project is to design and fabricate a wavemeter suitable for measuring the wavelength of visible, continuous wave laser emissions. After a review of the literature, a moving-arm Michelson interferometer was selected as the basis for the wavemeter. A twice folded path is used in the moving arm and electronic fringe rate multiplication is used in the counting circuit to improve system accuracy without increasing its overall size. A Z-80 based microcomputer is incorporated in the system for control and calculation purposes. Its use allows corrections to be made for the dispersion of air when the vacuum wavelength is calculated. Constraints on the wavemeter subsystems are derived from the basic design specifications. A description of the final design, including detailed information on the air rail, the fringe counting circuits, and the wavelength calculation algorithms, is presented. The portions of the wavemeter that were constructed are evaluated in regard to how well they meet the design specifications. Problems in stabilizing the frequency of the reference laser and amplifying the detected fringe signals prevented completion of the wavemeter. Recommendations are made concerning additional work that must be done to complete its fabrication.

I. Introduction

Since its invention over two decades ago, the laser has become a valuable laboratory instrument. A major role of the laser in the laboratory is as a source of narrow bandwidth radiation for use in spectroscopy. Ordinary discharge lamps have bandwidths on the order of 100 GHz and low-pressure isotope lamps have bandwidths of about 1 GHz (Ref 1:216). The range of bandwidths which can be found in different gas lasers is from on the order of 1 GHz (Doppler broadened) down to less than 10 MHz (an extremely stable laser) (Ref 2:55). A laser restricted to operating on one such narrow line is not as versatile as one capable of tuning over a range of such lines, such as a dye laser. With a tunable laser, though, means must be available to accurately determine the frequency at which the laser is oscillating. Techniques for measuring the wavelength using standard interferometers and spectrometers are often not convenient to use due to the time required to make the measurement. Most laser spectroscopists feel they would benefit from an instrument with the capability to rapidly measure wavelengths with an accuracy limited only by the linewidth of the laser (Ref 2:55). An instrument designed to accomplish this task is known as a wavemeter. Work has been done at many different laboratories towards developing practical, accurate wavemeters. Following a brief summary of the different approaches to wavemeter design that have appeared in the literature, the basic wavemeter design chosen for this

project is described.

Review of Previous Work

The different types of wavemeters that have been developed can be grouped into two categories: static and dynamic. The static wavemeters require no moving parts, other than adjustments for aligning or focusing, and can be used to measure the wavelength of either pulsed or continuous wave (cw) laser radiation. The dynamic wavemeters require at least one moving element in order to function and can be used only with cw signals. The static category includes the "sigma-meter," the multiple Fabry-Perot wavelength meter, and the Fizeau wavemeter. The dynamic category includes the scanning spherical Fabry-Perot and the Michelson wavemeters.

Static Wavemeters. The first wavemeter to be described in a scientific article was the French-developed sigma-meter (Ref 2:58; 3:438). It uses four Michelson interferometers with path differences of 0.05, 0.5, 5, and 50 cm. In operation, a small monochromater is first used to determine the integer order number of the smallest interferometer. Each interferometer is then used to determine the order number of the next longer interferometer. The accuracy is reported to be about 1 part in 10^8 (Ref 3:438). The primary problem with the sigma-meter is that it requires very difficult custom optical fabrication to avoid severe chromatic effects in the total internal reflection polarizing prism which is used to generate quadrature fringe intensities.

Another type of wavemeter has been under development at

Stanford University (Ref 4:414). This instrument contains three plane-parallel Fabry-Perot etalons. A grating monochromater is used to allow the desired wavelength to pass into the smallest etalon. Each etalon, from smallest to largest, is then used to determine the order number for the succeeding etalon. The determination of the order number is done using a vidicon tube and an electronic circuit. The accuracy is reported to be 1 part in 10^7 (Ref 4:415). The major problem with this wavemeter is its apparent overall complexity.

The final instrument in the static category is the Fizeau wavemeter developed at the National Bureau of Standards. This instrument uses a single Fizeau interferometer, a photodiode detector array, and on-line computer analysis to determine both the integral and fractional parts of the fringe order. The reported accuracy is to within a few parts in 10^7. The major problem with this wavemeter is due to systematic effects, such as beam shear, reducing the accuracy (Ref 2:60).

Dynamic Wavemeters. A wavemeter based on a scanning spherical Fabry-Perot interferometer has been developed at IBM. It requires a laser of known wavelength in addition to the laser whose frequency is to be determined. As the spherical Fabry-Perot is scanned over a distance of a few centimeters, the transmitted intensity of each of the two beams consists of a pulse train, with each pulse corresponding to a change of one in the order number. The ratio of the two

pulse train frequencies is inversely proportional to the laser wavelength ratio. The accuracy is reported to be 1 part in 10^7 (Ref 5:41). The major drawback to this wavemeter is that it is restricted to wavelengths well removed from the reference wavelength due to the technique used to start and stop the fringe counting (Ref 2:58).

Another dynamic wavemeter uses a Michelson interferometer with moving reflectors that change the difference in path length between the fixed arm and the variable arm of the interferometer. This type of wavemeter is probably the most commonly used (Ref 2:57). As with the scanning Fabry-Perot wavemeter, a reference laser is required and the unknown wavelength is calculated based on the ratio of the fringe counts for the two beams. A reasonably simple technique used to improve the precision of the instrument without increasing its size is to employ phase-locked frequency multiplication of the unknown laser signal to allow fractional fringes to be counted (Ref 6:367). Also, the beam path can be folded using corner cubes to give a greater effective path length change for the same amount of actual reflector movement. The accuracy with these improvements is reported to be 1 part in 10^8 (Ref 7:1611). A disadvantage of this wavemeter is that when only simple optical paths are used, a relatively long (~1 m) mirror motion is required in order to attain high accuracy (Ref 5:39). This type of wavemeter was chosen as the basis of the design in this thesis.

Problem Statement

The purpose of this thesis project is to design and fabricate a wavemeter which

a. Is capable of operating at any wavelength in the visible portion of the spectrum (400 to 700 nm).
b. Is accurate to at least 1 part in 10^6 (a few parts in 10^7 is desirable).
c. Automatically accounts for the dispersion of air in determining the vacuum wavelength.
d. Provides a digital readout of wavelength.
e. Is capable of operating autonomously, but has an interface to an external data collection computer.
f. Is as compact as possible.

Basic Wavemeter Design

The wavemeter design chosen for this project is based on the moving-arm Michelson interferometer. As explained in the theory chapter, this type of wavemeter can determine the unknown wavelength from the ratio of the fringe counts of the unknown wavelength and reference wavelength beams.

Figure 1 shows a simplified moving-arm Michelson wavemeter. Each laser beam is split into two portions which travel over different paths to reach the proper detector. When the two portions recombine at the detector, interference occurs. As the corner cube is moved, the length of one of the paths changes, and thus the phase relationship between the two portions of each beam changes. This changing phase relationship results in a series of interference maxima

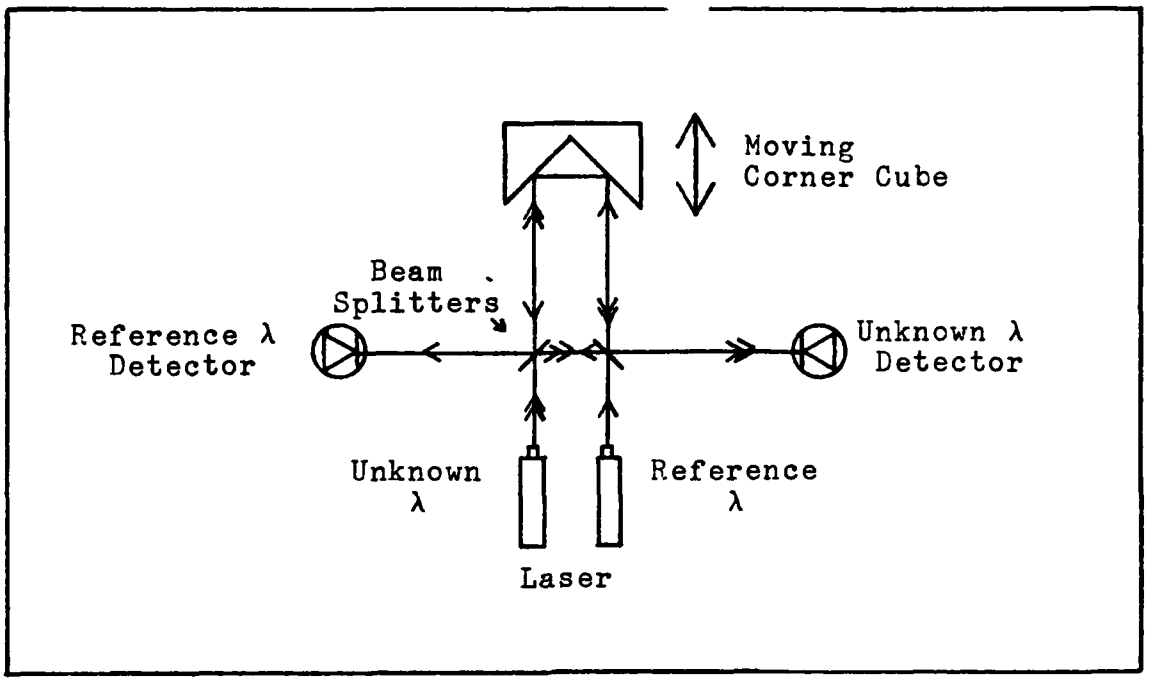

Figure 1. Simplified Moving-Arm Michelson Wavemeter

and minima (fringes) being generated. The ratio of the fringe counts produced at each detector as the corner cube is moved, along with the wavelength of the reference laser, is used to calculate the unknown wavelength (see Chapter II).

Scope

The lasers to be used with the wavemeter designed in this project will be operated in the cw mode. Thus, no provision is made for measuring the wavelength of pulsed lasers, since to do so would greatly complicate the design.

Assumptions

In the analysis of the sources of error in the wavemeter operation, the radii of curvature of the laser beam wavefronts are assumed to be large enough that the wavefronts can be approximated by plane waves. Corrections due to diffraction

of the laser beams are assumed to be much less than a few parts in 10^7 and can thus be neglected. This assumption is based on the small size of the laser beams (~3 mm) in relation to the size of the apertures in the beam path (~2 cm).

General Approach

A systematic approach was used in the design and fabrication of the wavemeter. The first step was to survey the literature to determine what types of wavemeters have been successfully used. Then, with the requirements specified for this project taken into account, a basic design was selected. The one selected was the dynamic Michelson wavemeter (Ref 2:57) incorporating a twice-folded moving beam path (Ref 7:1611) and electronic fringe rate multiplication (Ref 6:367). The next step was to design the various subsystems of the wavemeter. This included the designing of (1) an air rail to carry the moving reflectors, (2) the optical path of the interferometer, (3) fringe counting circuits, (4) control and calculation circuits which incorporate a microcomputer, and (5) the control circuits for stabilizing the frequency of the reference laser. As explained in Chapter IV, the design associated with stabilizing the frequency of the reference laser was not completed.

The design of the wavemeter components was not completed all at one time. Some portions were designed early on so that purchase orders could be mailed to commercial firms and work orders could be sent to the AFIT Model Fabrication Division in order to obtain required parts. As critical parts

were obtained, the next step, fabrication, was begun. As with the design, the fabrication of the wavemeter components was carried out throughout the duration of this project. The final step was to have been the characterization of the working wavemeter; however, since the wavemeter was not completed, no characterization could be done. Instead, an evaluation of the potential accuracy of the wavemeter was made.

Sequence of Presentation

A description of the design, fabrication, and evaluation of the wavemeter is presented as follows. First, the theory essential to understanding the operation of the wavemeter is presented. Next, the design requirements are analyzed. Following that, Chapter IV contains a description of the design of each of the wavemeter subsystems. Then Chapter V evaluates how well those portions of the wavemeter that were constructed meet the design requirements. Finally, Chapter VI presents the conclusions and recommendations that were made based on the results of the subsystem evaluation.

It should be noted that some implementation details have been omitted from the description of this thesis project. In particular, details on construction of the microcomputer are so well documented in Ref 8 that there is no need to reproduce them here. Also, a listing of the wavemeter program was omitted since much of it is not general enough in scope to be of interest to anyone who is not associated with the particular system fabricated in this project. However, flow charts describing the major routines are provided

(Appendix D). The omitted material has been compiled into a manual which is available to the operator of the wavemeter.

II. Wavemeter Theory

The wavemeter described in this report operates on the principle of the amplitude-splitting interferometer. It is a modified Michelson interferometer which incorporates simultaneous electronic fringe counting of two collinear laser beams. One of these beams is generated by the laser whose wavelength is unknown and the other, by a frequency stabilized reference laser. This chapter summarizes the theory underlying the operation of the wavemeter. The first section provides the theory essential to understanding interferometer operation (see also Refs 1:277-281; 9:184-189). It also includes the development of the equation which describes how the reference laser, its fringe count, and the fringe count of the unknown wavelength beam relate to allow the unknown wavelength to be calculated. The second section describes the theory associated with stabilizing the frequency of the reference laser.

Moving-Arm Interferometer

An interferometer operates on the principle that light waves from a single source traveling over two different paths to the same point will interfere, provided the optical path length difference is not greater than the source's coherence length. The total electric field amplitude at the point where the beams coincide will be equal to the sum of the two individual electric field amplitudes (Ref 1:276):

$$E = E_1 + E_2 \qquad (1)$$

Due to the very high oscillation frequency of optical radiation ($\sim 5 \times 10^{14}$ Hz), it is impractical to detect the electric field amplitude directly (Ref 1:277). Instead, the irradiance of the combined fields is normally detected by devices such as photodiodes. The irradiance, I, is proportional to the time average of the square of the magnitude of the electric field intensity and therefore contains a term which is the product of the two individual electric field terms. This interference term has the basic form (Ref 2:56)

$$N = 1 + \cos\left(\frac{2\pi \cdot \Delta l}{\lambda} + \phi\right) \qquad (2)$$

where Δl is the optical path length difference, λ is the wavelength, and ϕ is the phase difference between the two waves which would be present even if Δl were zero. Eq (2) indicates that the irradiance on the detector is a periodic function of Δl. As Δl changes by one wavelength, N goes through one complete amplitude cycle. The number of cycles N goes through as the optical path length is changed is also the number of wavelengths the path length was changed, or

$$\Delta l = \kappa\lambda \qquad (3)$$

where κ is the number of cycles or fringes. Thus, the wavelength of the beam can be determined by changing the optical path length by a known amount, counting the number of fringes detected, and calculating $\lambda = \Delta l/\kappa$.

The problem with this approach is in determining Δl to sufficient accuracy so that λ can be calculated accurately. One way of determining Δl accurately is to count the fringes produced by a known-wavelength beam. If this beam is

collinear with the unknown-wavelength beam, its fringe count can be used to calculate Δl using $\Delta l = \lambda_r \kappa_r$, where λ_r is the reference beam wavelength and κ_r is the reference beam fringe count. If while the reference laser fringes were being counted the fringes produced by the beam of the tunable laser (or as it will be called - the unknown laser) traversing the same path were also counted, the unknown wavelength (λ_u) could be calculated using

$$\lambda_u = \frac{\Delta l}{\kappa_u} \tag{4}$$

where κ_u is the fringe count for the unknown wavelength beam (or as it will be called - the unknown fringe count). Figure 1 in the previous chapter shows a simple system for accomplishing this.

This method assumes that the optical path lengths for the two beams are the same. This would be true if the wavelengths were identical or the transmission medium were non-dispersive. When the transmission medium is air and the wavelengths are different, the differences in the optical path lengths caused by the different indices of refraction at the two wavelengths must be accounted for. In this case

$$\Delta l = n\Delta L \tag{5}$$

where n is the index of refraction of air at the proper wavelength and ΔL is the physical path length difference. With this factor included, the wavelength of the unknown laser is found from Eqs (3) and (5) for the two wavelengths:

$$\lambda_u = \frac{n_u \cdot \Delta L_u}{\kappa_u} \tag{6}$$

$$\lambda_r = \frac{n_r \cdot \Delta L_r}{\kappa_r} \tag{7}$$

Solving Eq (7) for ΔL_r yields

$$\Delta L_r = \frac{\lambda_r \cdot \kappa_r}{n_r} \tag{8}$$

If the two beams travel the same path, then $\Delta L_u = \Delta L_r$ which allows Eq (8) to be substituted into Eq (6) giving

$$\lambda_u = \frac{\lambda_r \cdot \kappa_r \cdot n_u}{\kappa_u \cdot n_r} \tag{9}$$

Eq (9) summarizes the method described in this paper to determine λ_u. The ratio of the fringe counts from the reference and the unknown laser, modified to account for the dispersion of air (by n_u/n_r) and multiplied by the wavelength of the reference laser, produces the desired result. The method used to determine the individual terms of Eq (9) are described in later sections.

Longitudinal Zeeman Laser

The technique used to stabilize the frequency of the reference laser in this wavemeter uses the Zeeman effect. The following sections describe the Zeeman effect and how it can be used to stabilize the laser fequency.

Zeeman Effect. Zeeman splitting results when a magnetic field acts upon an atom's orbiting electrons. In the classical sense, this is caused by the force applied by the magnetic field adding to or subtracting from the angular velocity (ω) of the electrons. The orbits described by the electrons of an aggregation of atoms are oriented randomly in space.

When any one of these electrons is selected and its elliptical motion is broken up into three mutually perpendicular linear motions, the influence of the magnetic field can be examined. With the simplifying assumption that the electron is bound by an elastic force (F) obeying the law F = -br, where b is a constant and r is the displacement from the equilibrium position, the linear motions are simple harmonic motions (Ref 10:590). If a magnetic field is applied along one axis, two results can be noted. The first result is that the component of motion parallel to the magnetic field is unaffected, since it is equivalent to a current directed along the lines of force. The second result is that the other two components of motion cause the electron to move across the field and thus to be subjected to a force perpendicular to the field and its own motion. The net effect of this force is to change the two linear motions into two circular motions, one of higher frequency and one of lower frequency relative to the frequency of the original linear harmonic motion. Thus, the original elliptical orbit when subjected to a magnetic field is essentially transformed to a linear motion of unchanged frequency (f_o) along the field, plus two circular motions, one of higher ($f_o + \Delta f$) and one of lower ($f_o - \Delta f$) frequency, in the plane at right angles to the field (Ref 10:591). When observed parallel to the magnetic field, the component at f_o is not seen since this is equivalent to observing oscillating dipoles end-on, the direction in which no radiation is emitted. Thus, only two components are seen, one oscillating at $f_o + \Delta f$,

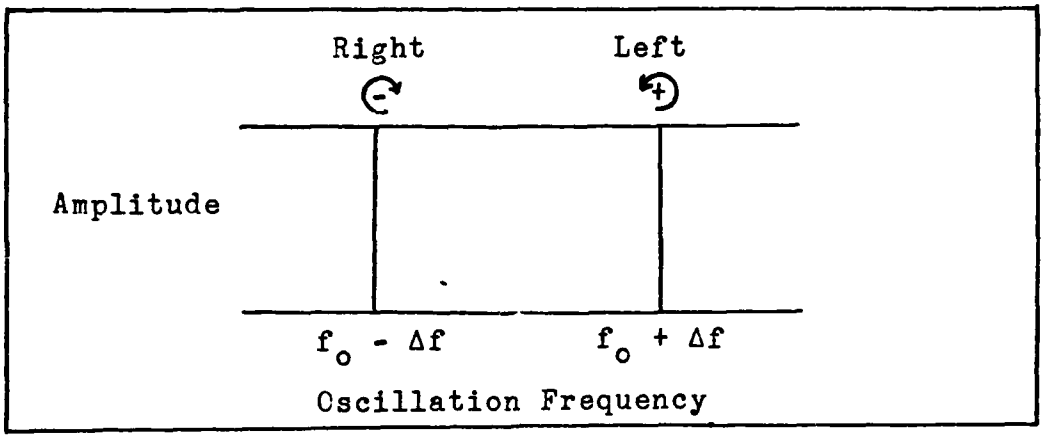

Figure 2. Zeeman Pattern (Viewed Parallel to Magnetic Field) (Ref 10:593)

with left-hand circular polarization, and one oscillating at $f_o - \Delta f$, with right-hand circular polarization (Ref 10:592). This is shown graphically as spectral lines in Figure 2.

In quantum mechanics, a shift in frequency of a spectral line implies a shift in the energy of one or both states involved in the transition. When placed in an external magnetic field, the energy levels change because of the energy of the atom's magnetic moment in the field. The number of allowed values of the magnetic quantum number (m), and thus the number of energy sub-levels, depend on the value of the angular momentum quantum number (l). There are 2l + 1 allowed values of m, ranging in value from -l to +l. Thus, an energy level with l = 1 would be split into three sub-levels by a magnetic field, with allowed m values of -1, 0, and +1. If such a split energy level were involved in a transition with an l = 0, and thus m = 0, energy level, three different transitions would be allowed, corresponding to $\Delta m = +1, -1$, and 0 . Transitions corresponding to $\Delta m = 0$

emit radiation of unaltered frequency (f_o) polarized parallel to the magnetic field, while transitions of $\Delta m = \pm 1$ emit radiation of altered frequency ($f_o \pm \Delta f$) which is circularly polarized when viewed parallel to the magnetic field direction (Ref 11:686). This is the situation when an electron of an excited neon atom drops from the 3S to the 2P level and emits 632.8 nm radiation (Ref 12:170). When such atoms are pumped within a stable resonator in a longitudinal magnetic field, an additional condition must still be met before laser oscillation will occur.

The condition that must be met is that for a stable mode the sum of the phase shifts for round trip propagation within the resonator must add up to zero. The standing wave frequency for a stable resonator is determined by

$$f = \frac{qc}{2nL} \tag{10}$$

where q is the cavity mode number, c is the speed of light, L is the cavity length, and n is the index of refraction of the medium. When the axial modes allowed by the characteristics of the laser cavity are considered, as a zero order approximation the two circular polarization components might be expected to oscillate with the same frequency since they are on the same resonator mode (Ref 13:474). The first order correction to this involves the different value of the index of refraction associated with each polarization. The dashed lines in Figure 3 show how the zero-field dispersion curve (not shown) splits into two separate curves, one for each

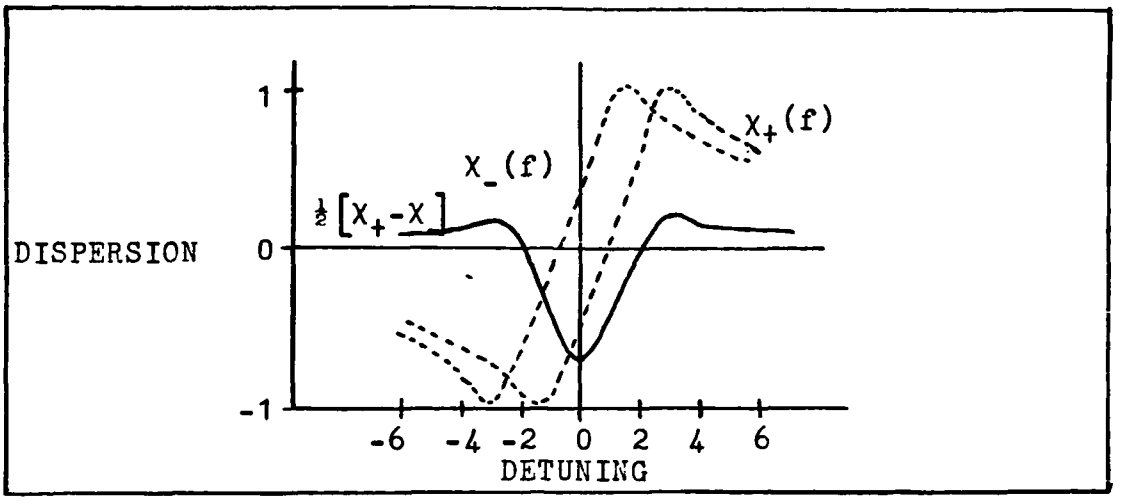

Figure 3. Dispersion for Left (χ_+) and Right (χ_-) Circularly Polarized Modes. (Ref 14:3174)

polarization. The dispersion is plotted as a function of detuning from line center (in arbitrary units). The split occurs due to the shift in the resonance frequencies of the different components of the atomic Zeeman doublet (Ref 14: 3173).

Beat Frequency Generation. If the two circular polarizations are mixed in a linear polarizer before being detected, the beat frequency corresponding to the difference frequency between the two modes can be observed. This beat frequency is given by (Ref 14:3174)

$$\Delta f = f_+ - f_- = \frac{qc}{2l}\left(\frac{1}{n_+} - \frac{1}{n_-}\right)$$

$$\propto f_o\left[\chi_+(f) - \chi_-(f)\right] \qquad (11)$$

where f_o is the zero magnetic field resonance of the cavity and $\chi_+(f)$ and $\chi_-(f)$ are the dispersion functions for the left and right circularly polarized waves. The difference between the dispersion functions for the left and right circularly

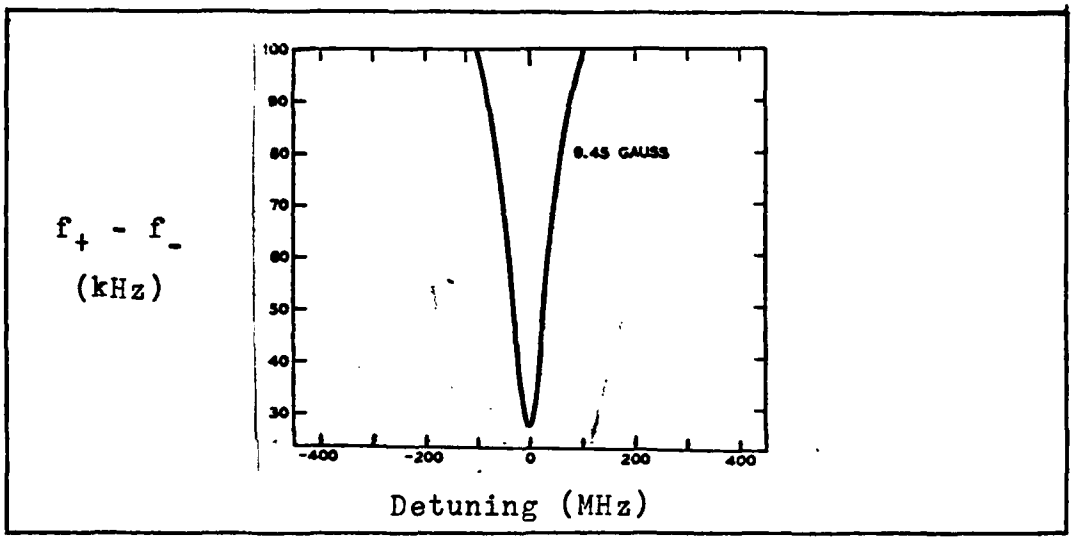

Figure 4. Beat Frequency vs Detuning from Line Center (Ref 13:473)

polarized standing waves is approximately proportional to the beat frequency. This difference is shown as the solid curve in Figure 3. Because of the symmetry of the magnetic field induced frequency shifts, the position of the central minimum of the difference curve in Figure 3 is independent of the magnetic field strength and is located at the line center. The actual value of this minimum frequency located at line center is directly proportional to the magnetic field strength (Ref 14:3174).

Figure 4 shows an experimentally derived curve of Δf as a function of detuning the resonator away from line center for a longitudinal magnetic field of 9.45 G. This characteristic of the longitudinal Zeeman laser, that is, the minimum in Δf which occurs when the resonator is tuned to line center, can be used as the basis for the stabilization of the laser frequency. Such a technique is described in Chapter IV.

III. System Analysis

Analysis of the general design requirements of this project indicates what specific features must be incorporated into the wavemeter. These general design requirements can be divided into two categories, the primary requirements and the secondary requirements.

Primary Requirements

The primary requirements are those which affect the basic operating capability of the wavemeter. These specify usable spectral range, accuracy, and size. They also require the instrument to be capable of self-contained operation.

Spectral Range. The specification on usable spectral range requires the instrument to be capable of providing air or vacuum wavelength readings for cw laser emissions throughout the visible portion of the spectrum. This means that all of the components used in fabricating the wavemeter must be suitable for use over that range of wavelengths. These components include both optical and electro-optical elements. The optical elements, the mirrors and beam splitters, must therefore have coatings which are effective over the visible spectrum. The electro-optical components, the fringe detectors, must have sufficient responsivity over the visible spectrum so that the fringe counting electronic circuits will have enough signal to work properly.

Accuracy. The accuracy specification requires the wavemeter readings to be accurate to at least within 1 part

in 10^6, but the accuracy goal is to be within a few parts in 10^7 (at 400 nm, 3 parts in 10^7 is equivalent to an error of 1.2×10^{-4} nm). To achieve this accuracy goal, certain design constraints must be placed on the wavemeter subsystems. These subsystems include the reference laser, the optical components, and the wavemeter electronics (fringe counting and calculation circuits).

The wavelength of the reference laser is critically important to the overall instrument accuracy since it is the basis for determining the wavelength of the unknown beam. Even if no other sources of error were present, the calculated wavelength could be no more accurate than the accuracy to which the reference wavelength is known. Thus, the reference laser wavelength must be stable and known to at least a few parts in 10^7.

The accuracy requirement also means the paths of the two beams through the movable portions of the wavemeter must be essentially identical. Since the reference laser fringe count (κ_r) directly affects the calculated wavelength (λ_u), the difference in the change in the path length of the reference laser beam from the change in the path length of the unknown laser beam must be small enough so the desired overall accuracy is achieved. This limits the amount the two beams can depart from being exactly collinear. Figure 5 shows two non-parallel rays representing the paths of the two beams. The extra distance one beam travels to reach the detector due to misalignment is represented by ε. The

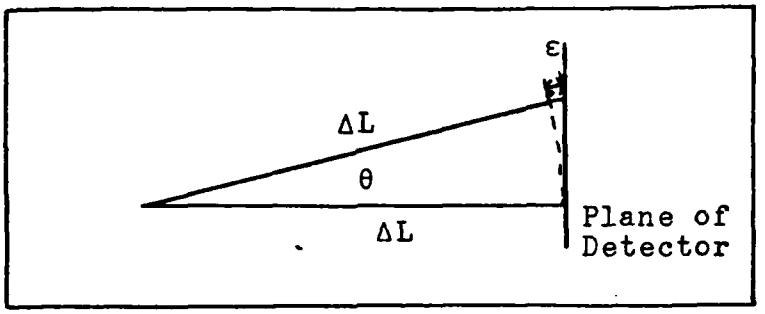

Figure 5. Path Length Difference for Non-Parallel Beams

allowed standard deviation for κ_r (σ_{κ_r}) to give a standard deviation of 1.2×10^{-4} nm for λ_u can be determined (Ref 15: 64-67). Given that $\lambda_u = (\lambda_r \cdot \kappa_r)/\kappa_u$ in a non-dispersive medium, then

$$\left[\frac{\sigma_{\lambda_u}}{\lambda_u}\right]^2 = \left[\frac{\sigma_{\lambda_r}}{\lambda_r}\right]^2 + \left[\frac{\sigma_{\kappa_u}}{\kappa_u}\right]^2 + \left[\frac{\sigma_{\kappa_r}}{\kappa_r}\right]^2 \qquad (12)$$

where σ denotes the standard deviation of the quantity which is its subscript. If σ_{λ_r} and σ_{κ_u} are both zero, then

$$\sigma_{\kappa_r} = \frac{\sigma_{\lambda_u} \cdot \kappa_r}{\lambda_u} \qquad (13)$$

If λ_u = 400 nm (worst case), $\sigma_{\lambda_u} = 1.2 \times 10^{-4}$ nm, and κ_r = 2,097,152 (as determined in Chapter IV), then σ_{κ_r} = 0.83 fringes. The given value of κ_r equates to a path length change (ΔL) of 1.327 m (for λ_r = 632.8 nm). The maximum angle allowed between the two beams in order to keep σ_{κ_r} < 0.83 fringes (θ in Figure 5) is given by

$$\theta = \cos^{-1} \frac{\Delta L}{\Delta L + \varepsilon} \qquad (14)$$

where $\epsilon = \sigma_{\kappa_r} \cdot \lambda_r$. For the constants given above, θ must be less than 0.89 mrad to ensure the desired system accuracy is achievable. Over a three meter path this is equivalent to a 2.7 mm misalignment. As indicated in Chapter IV, a technique is used whereby the number of fringes is multiplied by 20 in order to count fractional fringes. For this multiplication scheme to be meaningful, the actual allowed misalignment must be 20 times less than that given above, or 0.14 mm. It must be noted that this calculation assumes that the radii of curvature of the wavefronts in the laser beams are large enough so that the waves can be approximated by plane waves.

Eq (12) can be used to determine the accuracy required of the fringe counting circuits, which, for σ_{λ_r} and σ_{κ_r} both equal to zero, gives

$$\frac{\sigma_{\kappa_u}}{\kappa_u} = \frac{\sigma_{\lambda_u}}{\lambda_u} \simeq 3 \times 10^{-7} \qquad (15)$$

If the error in κ_u is 1 count, then κ_u must be on the order of 3.3×10^6 counts. If the error in κ_u is larger than 1 count, then κ_u must be made larger by an equal multiple to keep the overall accuracy the same.

Since the accuracy requirement must be met over the entire visible portion of the spectrum, Eq (5) must be examined to determine what impact the dispersion of air will have. If only the wavelength in air were required, no correction for the air dispersion would have to be made since it would already be accounted for in the fringe counts. This can be shown from Eq (5) and $\lambda_{air} = \lambda_{vac}/n$ which,

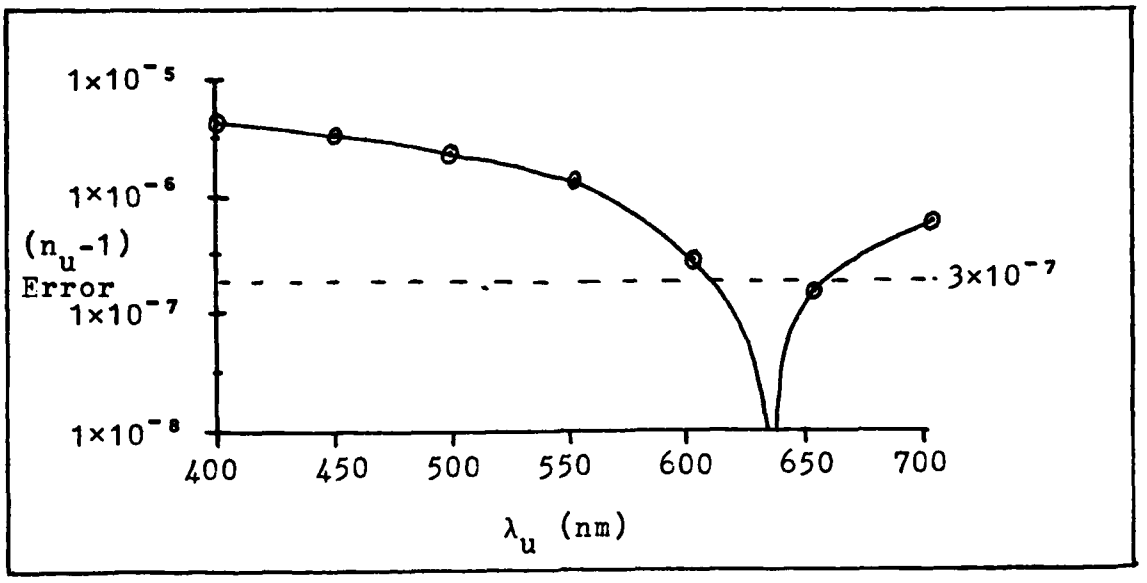

Figure 6. Error in n_u vs λ_u (Ref 16 used as source for n_u)

when combined, results in

$$\lambda_{u,a} = \frac{\lambda_{r,a} \cdot \kappa_u}{\kappa_r} \tag{16}$$

where the additional 'a' subscript indicates the value in air. When the vacuum wavelength is considered, the full Eq (5) must be used. With terms added to Eq (12) for the standard deviations of the indices of refraction, the allowed error in n_u can be determined. If the only error present is due to n_u, the applicable equation is

$$\sigma_{n_u} = \frac{\sigma_{\lambda_u} \cdot n_u}{\lambda_u} \tag{17}$$

If λ_u = 400 nm, $\sigma_{\lambda_u} = 1.2 \times 10^{-4}$, and n_u = 1.000282749 (Ref 16:201), then the allowed value for σ_{n_u} is 3.0×10^{-7}. Figure 6 shows how the fractional error in n_u varies as a function of λ_u when n_u is assumed to be equal to n_r. The

conclusion from this is that to meet the accuracy criterion, corrections for the dispersion of air must be made. In doing so, two factors must be considered. The first is the dispersion caused by standard dry air, that is, air at 15° C and 760 mm Hg pressure with no water vapor content. This can be calculated using Edlén's formula (Ref 16:iv):

$$n = 1.0 + 6432.8 \times 10^{-8} + \frac{2{,}949{,}810}{146 \times 10^{8} - \nu^2} + \frac{25{,}540}{41 \times 10^{8} - \nu^2} \quad (18)$$

where n is the index of refraction of standard dry air and ν is the vacuum wavenumber in cm^{-1} with

$$\nu = \frac{1}{\lambda_{vac}} = \frac{1}{n \cdot \lambda_{air}} \quad (19)$$

The second factor to be considered is the correction to n which accounts for nonstandard conditions. An emperical formula for this correction has been determined (Ref 16:iv):

$$(n'_{t,p,w} - 1)10^6 = \frac{(n - 1)10^6}{720.8826} \times \frac{p\{1 + (1.049 - 0.0157t)p \times 10^{-6}\}}{1 + 0.003661t} - \left[0.0624 - \frac{0.0680}{\lambda^2}\right] \frac{w}{1 + 0.003661t} \quad (20)$$

where $n'_{t,p,w}$ is the index of refraction at nonstandard temperature (t), pressure (p), and water vapor (w) and n is the index at standard conditions found using Eq (18). To determine the impact this correction would have on the calculated value of λ_u, n′ was calculated for several values of t, p, and w at different wavelengths in the visible spectrum. In

the worst case (λ_u = 400 nm), the correction [for t = 20° C, p = 780 mm Hg and w = 15 mm Hg (warm, humid air)] involves multiplying n_u by 1.000001606 to get n′. Since Eq (5) uses the ratio of n_u to n_r and the correction to n_r (for λ_r = 632.8 nm at the same conditions) is 1.000001552, the overall correction to λ_u is on the order of 2×10^{-5} nm. Since this is almost an order of magnitude smaller than the desired accuracy, it can be neglected; thus, all calculations will be made for standard dry air conditions.

In order to maintain the required accuracy, the method used to calculate Eqs (9) and (18) must have sufficient precision. The degree of precision required is determined by the values used in the calculations, that is, the number of significant digits that must be carried to meet the accuracy requirements. Since the calculations will be done using binary arithmetic, a lower bound is thus set on the number of significant bits used in the calculation scheme. The calculation scheme must also be capable of processing the range of magnitudes that can occur in the equations. From the given constants and variables of the two equations, the minimum number of significant bits must be 24. This was determined by converting the constants and worst case values for the variables into normalized floating point format and selecting the one which requires the most significant bits. The maximum absolute magnitude of the numbers involved in the calculations is 10^8. A seven bit floating point exponent, including one bit for the sign of the exponent, is the

minimum required.

Size. The size specification requires the wavemeter to be as compact as possible so that the optical components can be easily accomodated on an optical table with other instruments. This specification mainly impacts the number of fringes that can be counted by limiting the amount of path length change that can be achieved. For the worst case (λ_u = 700 nm), to get $\kappa_u = 3.3 \times 10^6$ counts as specified in the previous section on accuracy, would require a path length change of 2.3 m (from $\Delta l = \kappa_u \cdot \lambda_u$). In order to keep the instrument size reasonable, while the desired accuracy is maintained, some method must be used to achieve the required fringe count without actually using this much space. Two ways to do this are described in the design chapter. For the purpose of this section, the limit on size means the wavemeter will require a more complicated beam path, and thus more optical elements, and more complex electronic circuits in order to achieve the required accuracy.

Self-Contained Operation. The requirement that the wavemeter be capable of self-contained operation means it cannot rely on an external computer in any way. This means the wavemeter must be capable of doing all of the required calculations. Because of the magnitudes and range of the values involved in the calculations, some form of computer support is required. Thus, the wavemeter must incorporate a microcomputer which has been programmed to do the required operations.

Secondary Requirements

The secondary requirements are those which do not impact the basic operating capability of the wavemeter, but do affect the ease with which it can be incorporated into the laboratory. These require that the wavemeter operate automatically, that it interface easily with the laser it will primarily be used with, and that it communicate with the laboratory general purpose computer.

Automatic Operation. The specification requiring automatic operation means that, after the unknown wavelength beam is initially aligned with the system, no further intervention by the operator will be required to provide a periodically updated display of the laser's operating wavelength. The discussion in the section on accuracy requirements has already assumed that the calculations associated with the wavemeter operation would be done in some automatic manner instead of just displaying the fringe counts and letting the operator do the remainder of the work. The other components of the wavemeter that must be automatic are those which move the reflector to change the optical path length of one arm of the wavemeter and which count the fringes thus generated. An arrangement must be made to automatically reset these components at the end of one calculation and restart them for the next. Also, the quality of the fringes, that is, their visibility, must be great enough for the fringe counting circuit to be able to distinguish one fringe from another. For proper operation, the counting circuit must be able to recognize the difference between two voltage levels corresponding to the

interference maximum and the adjacent minimum. In the ideal case, when the visibility (V) is unity, the minimum is zero, since

$$V = \frac{I_{max} - I_{min}}{I_{max} + I_{min}} \tag{21}$$

where I_{max} and I_{min} correspond to the irradiances at fringe maxima and minima, respectively. As the difference between I_{max} and I_{min} decreases, the visibility decreases which makes the fringes less well defined and harder to detect. The major factor which determines fringe visibility for interference between two mutually coherent waves is the relative irradiances of the two waves at the point of interaction. The total irradiance at this point is (Ref 1:278)

$$I = I_1 + I_2 + 2\sqrt{I_1 I_2} \cos \delta \tag{22}$$

where I_1 and I_2 are the irradiances of the individual waves and δ is the phase difference between them. For an interference maximum, δ must be an even multiple of π; for a minimum, it must be an odd multiple. Thus,

$$I_{max} = I_1 + I_2 + 2\sqrt{I_1 I_2} \tag{23}$$

and

$$I_{min} = I_1 + I_2 - 2\sqrt{I_1 I_2} \tag{24}$$

If Eqs (23) and (24) are substituted into Eq (21) and simplified, the resulting equation is

$$V = \frac{2\sqrt{I_1 I_2}}{I_1 + I_2} \tag{25}$$

When the irradiances of the two beams are equal, the visibility is a maximum, provided Δl is much less than the coherence

length of the source. As the irradiance of one beam decreases relative to the other, the visibility decreases. For the wavemeter design this means the difference between the attenuations introduced in the two different beam paths must be small enough to ensure sufficient fringe visibility at the detectors.

Ease of Interface. The interface specification requires that the wavemeter be constructed such that as few optical elements as possible will be required to couple in the unknown wavelength beam from a cw dye laser such as the Spectra Physics Model 375. This laser is the primary one with which the wavemeter will be used. Although the height of the Model 375 laser can be adjusted slightly, if the beam path within the wavemeter is made to be 9.75 inches above the table, only a turning mirror should be required to interface the unknown beam with the wavemeter.

Computer Link. The requirement that the wavemeter be able to communicate with the laboratory general purpose computer means the wavemeter must have a suitable communications link to this computer and that it be able to send the wavelength data over this link in a format compatible with the computer's interface. The general purpose computer is a Digital Equipment Corporation LSI-11 which is presently configured with an RS-232 serial data port. Thus, to be compatible the wavemeter must send its data in a serial format (eight bits per character) following RS-232 signal protocols.

IV. Design

The design of the wavemeter was completed in two stages. The first stage involved the selection of a general design for the wavemeter which would meet the specified requirements. The second stage included the design of each of the wavemeter subsystems. This chapter presents the pertinent aspects of these two design stages.

General Design

The first step in the general design stage involved a literature search to determine what types of wavemeters have been reported on in the past. A summary of what was found was described in Chapter I. Next, in order to select which should be used, the various wavemeter designs were compared with the established requirements. It was determined that each wavemeter type except the scanning Fabry-Perot could meet all of the requirements. The scanning Fabry-Perot wavemeter failed to meet the requirement on usable spectral range due to its limitation of use at wavelengths well removed from the reference laser wavelength (Ref 2:58). From those that did meet all of the requirements, the final selection was made based on an estimation of the ease of instrument construction and parts acquisition. The design which appeared to best fit these considerations was the dynamic, or moving-arm, Michelson wavemeter. Thus, it was chosen as the basis for the instrument designed in this thesis.

Subsystem Design

In the subsystem design stage, the various parts which make up a dynamic Michelson wavemeter were designed. Based on descriptions in the literature, the major subsystems were determined to be the following: the reflector drive subsystem, the beam path subsystem, the electronics subsystem, and the reference laser subsystem. The design of each of these subsystems is described in the following sections.

Reflector Drive Subsystem. The purpose of the reflector drive subsystem is to automatically and smoothly move the reflector in the moving arm of the interferometer so that a series of fringes are generated at the detectors. The length over which the reflector must travel is determined by the desired instrument accuracy in conjunction with the configuration of the beam path. For a given beam path configuration, if the length of travel in the moving arm of the interferometer is increased, the accuracy to which the wavelength can be determined is increased, at least up to the point where other factors start limiting the accuracy. In order to limit the size of the wavemeter, a twice folded beam path is used in the moving arm as described in the next section (see Figure 7). This means that for a given movement of the reflectors, the beam path length changes by four times as much. In the accuracy section of Chapter III, the required minimum fringe count was determined to be 3.3×10^6, for $\sigma_{\kappa_r} = 1$. With the twice folded beam path, this means the reflector in the moving arm must be capable of being moved

$(3.3 \times 10^6 \cdot 700 \times 10^{-9})/4 = 57.7$ cm. As described in a later section, electronic fringe multiplication is used to help reduce the system size. This allows a smaller value for the minimum count, $\sim 2.1 \times 10^6$, to be used. To generate this number of fringes, the reflector must be moved 36.7 cm. To allow a margin of error, the V-rail was made long enough (59 cm) to allow the reflector to be moved 39 cm between the optical switches. As the reflector moves over this distance excessive vibrations must be avoided to keep from creating extraneous fringes.

To minimize vibration-induced extraneous fringes, an air cushioned slide is used to move the reflector. Originally, a commercial air track was to be used with a motor driven chain providing the motion; however, due to logistics problems, local fabrication of a suitable air track was required. The design selected, based on one developed at the National Bureau of Standards (Ref 17), is in the "inverted" configuration in which the air is fed to the slide (the air bearing) rather than the V-rail. The advantage of the inverted configuration is that the escaping air generates considerably less turbulence in the air the beam passes through. Appendix A contains details of the air bearing construction.

To allow the wavemeter to operate continuously without operator intervention, a method is required to reverse the direction of motion of the air bearing when it reaches the end of the V-rail. Simple springs would provide the needed direction change, but due to their energy losses, would

eventually damp out the motion of the air bearing. To replace the energy lost in the springs, a solenoid and trip switch were installed at one end of the V-rail. The trip switch is built into the tip of the solenoid plunger and the spring is coiled around the plunger. By varying the voltage on the solenoid and the extent to which the plunger extends into the spring coil, the amount of energy imparted to the air bearing can be controlled. Photoelectric switches ("optical switches") signal the wavemeter electronics when the air bearing is no longer in contact with the springs so that fringe counting can begin.

Beam Path Subsystem. The purpose of the beam path subsystem is to guide the reference and the unknown laser beams around the two paths of the Michelson interferometer. This subsystem is made up of seven optical elements, five mirrors and two beam splitters, each in an adjustable mount. The basic layout for the beam path (Figure 7) is modeled after the improved wavemeter of Ref 7. The main consideration in selecting this layout was its potential for high accuracy while maintaining an overall small size by using a twice folded path in the moving arm. Another consideration was to keep the two beam paths similar to each other. That is, when they reach the detector, the size and irradiance of each of the beams should be nearly identical. This requires both similar path lengths for the two beams and equal division of the beam energy at the beam splitters. This was necessary to keep the visibility high enough to allow the fringes to be

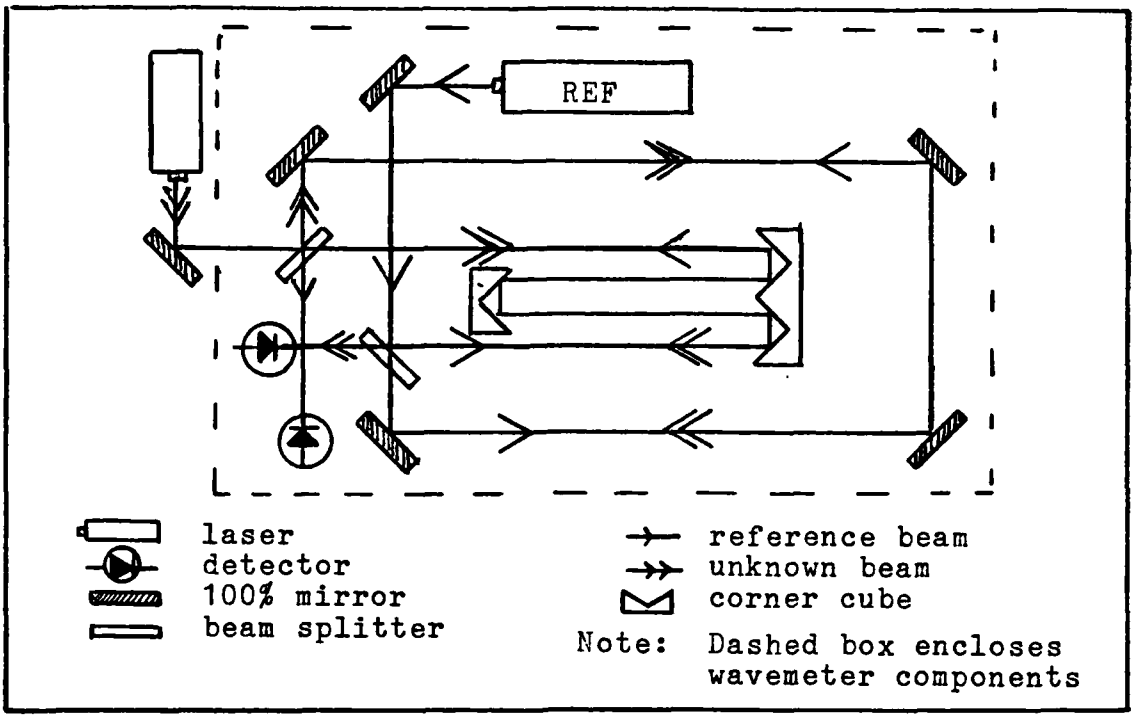

Figure 7. Beam Path Layout

counted. Also, the optics must be usable over the entire visible spectrum. The one exception to this is the turning mirror for the reference beam.

The alignment of this subsystem is critical to accurate operation of the wavemeter as indicated in Chapter III. In order to make this alignment easier, the height of the beam path above the table top was matched to the height of the Spectra Physics Model 375 dye laser, the primary source of the unknown laser beam. This eliminates the need for a pair of mirrors to raise or lower the beam height to match the wavemeter. Thus, once the beam path subsystem is aligned so the two parts of the reference beam remain collinear, the unknown beam only has to be aligned with the reference beam.

Electronics Subsystem. The purpose of the electronics

subsystem is to convert the interference fringes generated at the detectors into electrical signals which it then manipulates and finally displays as the wavelength of the unknown laser beam. To accomplish this, several different functions must be performed. First, the irradiance variations which occur in each of the laser beams due to interference (the fringes) must be converted by a detection circuit into electrical signals which are compatible with the rest of the electronics subsystem. Second, the interference fringes in the form of these pulsed electrical signals must be counted. Third, these two fringe counts must be manipulated using the appropriate equations [mainly, Eqs (9), (16), and (18)] given in Chapters II and III to calculate the unknown wavelength. Finally, the calculated wavelength must be displayed to the operator and sent over a communications link to an external computer for data collection. Figure 8 shows how these different functions are connected together. Each of the functions is described in the following paragraphs.

The detection circuit acts as the transducer between the interference fringes of both the reference and the unknown laser beams and the rest of the electronics subsystem. The first stage of this circuit is the detectors which generate electrical signals proportional to the irradiance from the laser beams. Two detectors are required, one for the reference beam and one for the unknown beam. Neither detector is required to have an extremely fast response since the fringe generation rate is on the order of 1 MHz. This is calculated

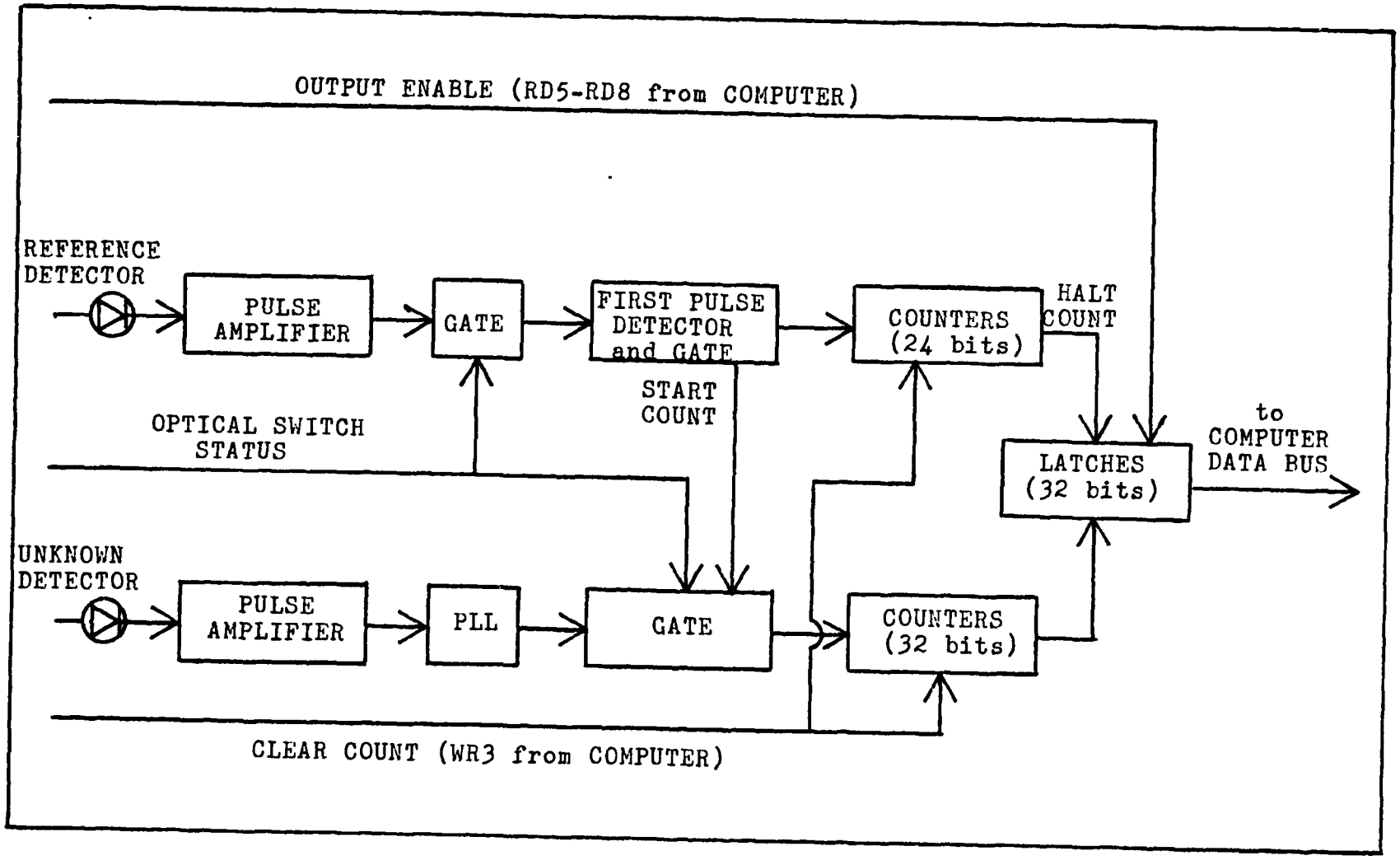

Figure 8. Electronics Subsystem Block Diagram

using the amount of path length change the moving reflector will induce, the time required for this movement (t), and the wavelength of the laser. For the worst case, λ = 400 nm, the fringe rate is

$$\frac{\Delta l}{\lambda \cdot t} = \frac{1.47}{400 \times 10^{-9} \cdot 2.75} = 1.34 \text{ MHz} \qquad (26)$$

The detector for the reference beam is only required to respond at 632.8 nm; however, the detector for the unknown beam must respond over the entire visible range. The detector chosen for both purposes was the EG&G Model FND-100 silicon photodiode. Figure 14 (Appendix B) contains data on this detector's spectral and temporal response.

The low current output of the detectors must be modified to match the voltage levels required by the subsequent circuits. Since the subsequent circuits use transistor-transistor logic (TTL), the required voltage levels are 0 - +0.4 v for a logic zero and 2.4 - 5.0 v for a logic one (Ref 18:63). The logic zero level corresponds to a fringe minimum and the logic one, a fringe maximum. As indicated in Chapter VI, the portion of the detector circuit used to condition the signal for the subsequent circuits was not completed; however, discussion in the remainder of this section assumes the pulse trains are available at the proper voltage levels. These TTL level pulses drive the next portion of the electronics subsection, the fringe counting circuits.

The fringe counting circuits convert the TTL level pulse trains into binary number representations of how many

fringes have been formed at the detector. Two separate counting circuits (channels) are used as shown in the block diagram in Figure 8 and schematic diagram in Figure 15 (Appendix C). The two channels are basically identical except that the one which counts the unknown fringes has incorporated into it a phase-locked loop (PLL) to multiply the fringe rate by 20 to increase the wavemeter accuracy. Multiplying the fringe rate prior to counting the fringes in effect allows fractional fringes to be counted. Thus, instead of an average error of 0.5 counts in about 2 million counts (2.5×10^{-7}), the average error will be on the order of 1 count in about 40 million counts (2.5×10^{-8}). This assumes that the PLL voltage controlled oscillator (VCO) successfully tracks any changes in the fringe rate caused by changes in the speed of the moving reflector. The second channel, which counts the reference fringes, synchronizes the initiation of the counting cycle for both channels to the occurrence of the first reference pulse through the gate. This channel also controls the end of the counting cycle. It is wired so that when its count reaches a preset number, the counting of the multiplied reference fringes is halted. The preset number is selected so that even in the worst case (λ = 700 nm) the count will be completed before the air bearing triggers the optical switches at the ends of the V-rail. Thus, for a reflector travel of 39 cm between the optical switches, the preset count must be less than 2.22×10^6. Since the counting is done in binary, 2^{21} (which is 2,097,152 in decimal

notation) was selected to make the end-of-count decision logic simple. At the end of the count sequence, the final unknown fringe count is automatically loaded into four tri-state latches. These latches can be accessed by the wavemeter's microcomputer.

The microcomputer calculates the unknown wavelength and performs all of the control and data output functions required for the wavemeter. Use of a microcomputer in the wavemeter was dictated primarily by the requirement that when the vacuum wavelength is calculated, a correction for the dispersion of air must be included. This would be impractical using discrete logic, and the use of an external computer was not allowed in the design specification. Also, the use of the microcomputer will allow improvements to be incorporated into the wavemeter in the future with the relative ease of only reprogramming, rather than re-wiring discrete logic. The microcomputer used in this thesis project was constructed by Rogers and Ross (Ref 19) using the design in Ref 8. For proper wavemeter operation, the microcomputer must (1) recognize when a counting sequence is completed, (2) read the unknown count from the tri-state latches, (3) determine if the operator wants the air or the vacuum wavelength calculated, (4) calculate the wavelength with sufficient precision, and (5) output the calculated wavelength to both a display and an external computer. Figure 19 (Appendix D) shows the task sequence for the microcomputer. The methods used to accomplish these tasks will now be described.

The microcomputer determines when a counting sequence is completed from the status of the optical switches located at the ends of the V-rail. Since the counting sequence is always completed before the optical switches change state, such a change in state is a valid indicator that the microcomputer can use. For detecting this state change, a control line is connected from the optical switches to one of the microcomputer's input ports. Figure 9 shows this connection. When the voltage on this line represents a logical zero, the microcomputer begins the program sequence to calculate the unknown wavelength.

The first step in the calculation sequence is to transfer the unknown count from the tri-state latches into the microcomputer's memory. The microcomputer does this by treating each of the four latches as an input port and doing a read from that port. Figure 9 shows these connections. The next step in the calculation sequence is to determine whether the operator wants the air or the vacuum wavelength calculated depending on the setting of the front panel selection switch. The microcomputer does this by treating the control line from the switch as an input port and doing a read from that port (see Figure 9). A logical one on that line indicates the air wavelength calculation has been selected. The final step in the calculation sequence is to calculate the selected wavelength. Eqs (9), (16), and (18) are the main ones used in this portion of the program. Flow charts for the air wavelength and the vacuum wavelength

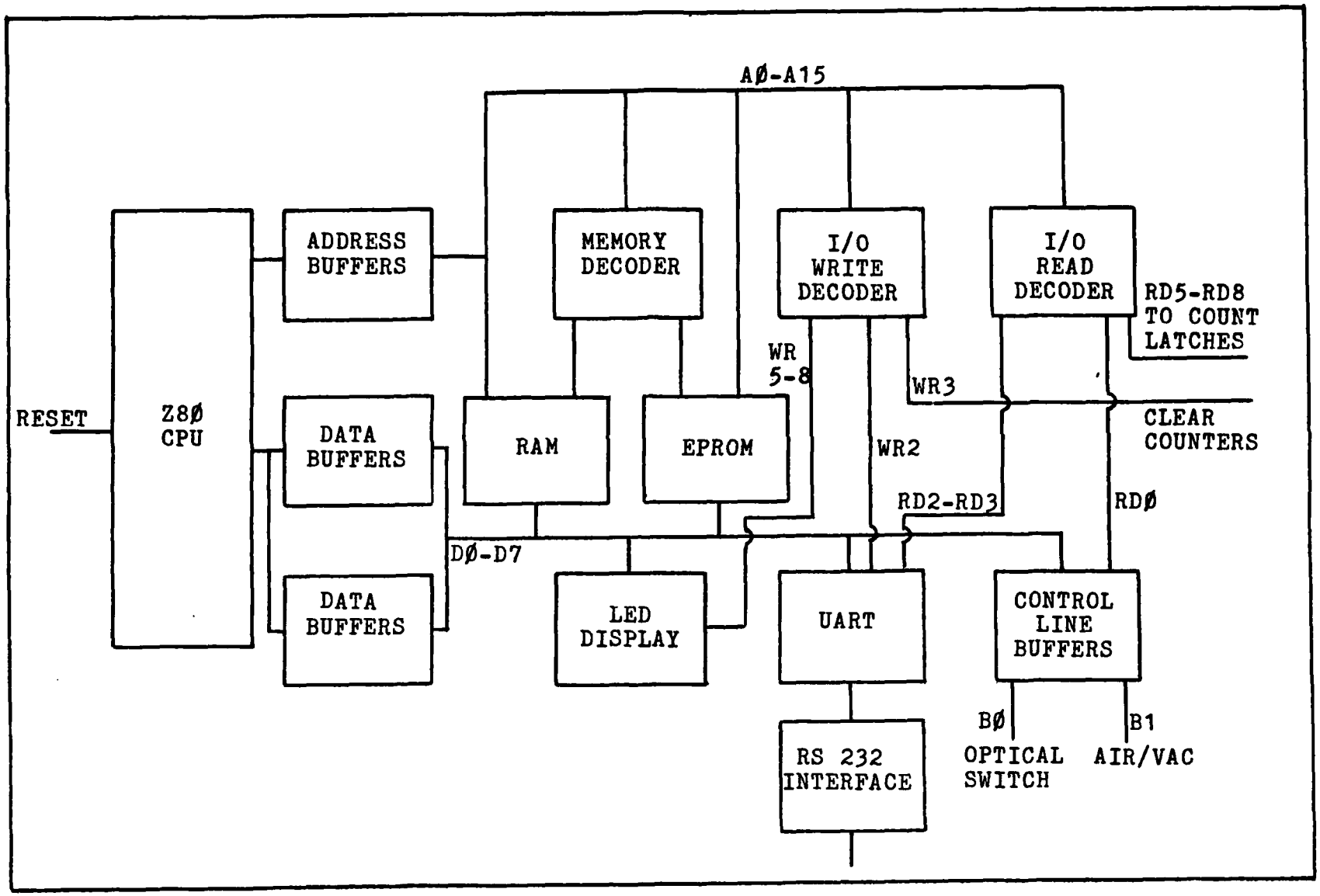

Figure 9. Microcomputer Block Diagram

calculation sequences are contained in Appendix D. To meet the accuracy requirement, the calculation must be done with 24 significant bits and 6 bits of exponent. The most practical way for these calculations to be done with the 8-bit Z80 based microcomputer is by the use of a signed floating point format with four bytes for the mantissa and one byte for the exponent. The format used is as follows:

sbbbbbbb	bbbbbbbb	bbbbbbbb	bbbbbbbb	sbbbbbbb
MSB	NSB	NNSB	LSB	EXP
	mantissa			exponent

where

MSB = most significant byte
NSB = next most significant byte
NNSB = second next most significant byte
LSB = least significant byte
EXP = exponent
b = bit
s = sign bit

The multiple precision arithmetic subroutines used in the wavemeter's assembly language program were adapted from Ref 20.

The final wavemeter function is to output the calculated wavelength. This is done in two ways. The first way is by the microcomputer sending the wavelength to the LED display on the front panel of the wavemeter. It does this by converting the floating point representation of the wavelength into binary coded decimal (BCD) form. The BCD digits are packed by pairs into bytes (8-bits per byte). These pairs of digits correspond to adjacent digits on the display. Each pair of adjacent display digits is treated as an output port and the microcomputer writes the appropriate byte of data to

it. Figure 9 shows these connections. The second way the data is output is by the microcomputer transmitting each of the five bytes of the wavelength's floating point representation over the RS232 interface.

Reference Laser Subsystem. The purpose of the reference laser subsystem is to provide a stable and accurately known wavelength for use in calculating the unknown wavelength. The reference laser used in the wavemeter will be stabilized in frequency using the longitudinal Zeeman effect. The theory of this effect was described in Chapter II. The specifics of its use in frequency stabilization are based on the method used in Ref 14. For the reason described later in this section, fabrication of this portion of the wavemeter was not completed.

The beat frequency between the two circularly polarized modes described in Chapter II can be used as an error signal to indicate when the laser is tuned to the center of the Doppler broadened line. This can be done using the arrangement shown in Figure 10. The dither signal is applied to a piezoelectric transducer (PZT) which is mounted so that it will apply an axial force to the laser tube. This force will stretch the tube slightly and change its resonant frequency with respect to line center. This causes the beat frequency to change. A change away from line center in either direction causes the beat frequency to increase. A reversible counter used to count at the beat frequency can generate an error signal in the following way. If the laser

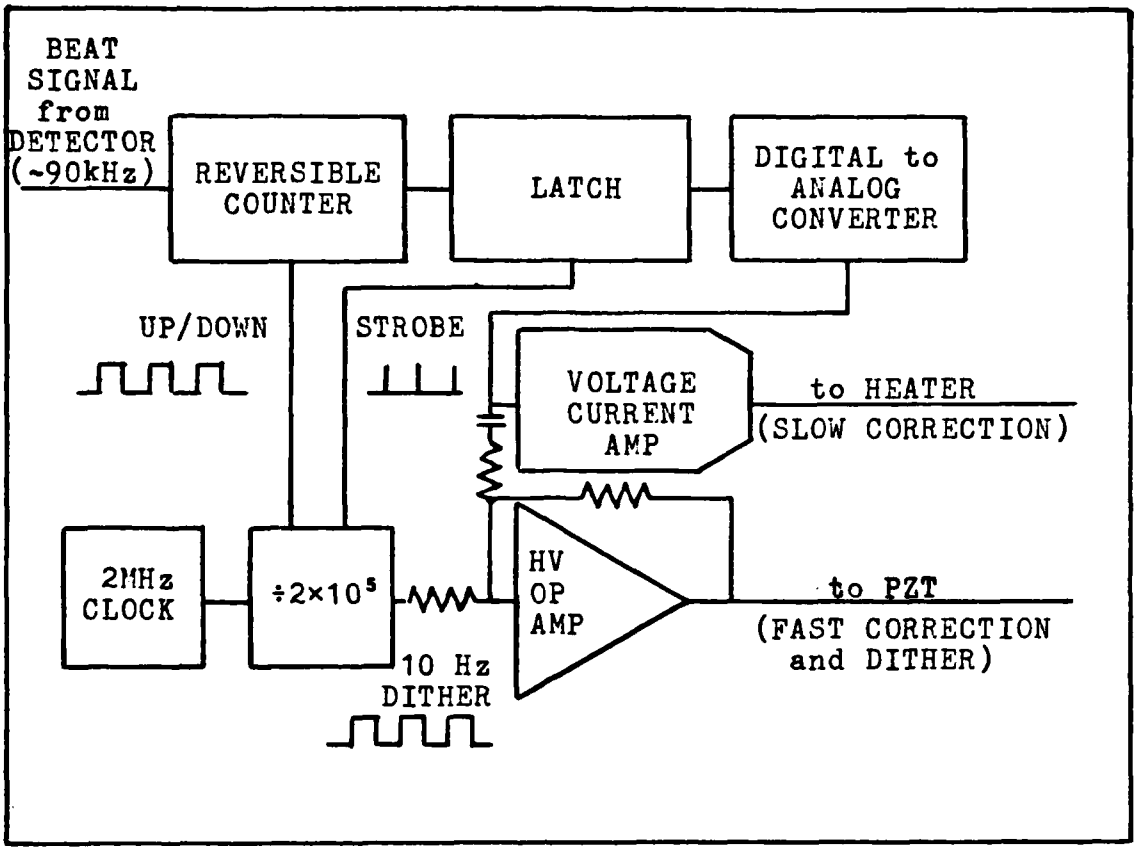

Figure 10. Zeeman Stabilization Scheme (Ref 14:3175)

is tuned to line center and the reversible counter counts up when the dither signal shifts the laser frequency up, and counts down when the dither signal shifts it down, the net count will be zero. If the laser frequency drifts in either direction, a non-zero net count will remain after each dither cycle. This count will indicate in which direction the laser must be tuned to return its frequency to line center. The fast correction for the drift is supplied by the PZT. The slow, or long term, correction is provided by the digital to analog converter and the heater circuit, which includes a length of nichrome wire wound around the plasma tube. Figure 16 (Appendix C) is a schematic diagram of the reversible

counter portion of this subsystem.

The selection of the laser tube to use in this subsystem was governed by two main factors: (1) the tube had to use a sidearm internal mirror cavity so the PZT could be attached as required, and (2) the tube had to be one of those already on hand. The selected tube was a Spectra Physics Model 060-2 used in their Model 132 HeNe laser. An unsuccessful attempt was made to operate this laser on a single longitudinal mode by limiting the current supplied to the anode. At a current of 2.5 ma the plasma became unstable, but even up to that point two modes were still present as indicated on the display of a scanning Fabry-Perot etalon. The second mode was an order of magnitude lower in amplitude than the main mode. For this reason, it was decided that it would be possible to stabilize the laser using the main mode, and that the secondary mode would have negligible effect on the fringe counting accuracy as long as the main mode remained near the line center.

To determine the effect this additional mode would have on the stabilization circuit, the beat frequency between the two circular modes was detected and observed. The signal emitted through the rear mirror of the cavity was passed through a polarizing prism into a detector. The detection circuit used an EG&G HAV-1000A silicon photodiode/amplifier combination. Figure 17 (Appendix C) is a schematic diagram of this circiut. The amplified signal was monitored on an oscilloscope. The behavior of the beat signal was as described in Chapter II, that is, the minimum frequency

occurred when the line was centered under the gain curve and was dependent on the magnetic field strength. With two bar magnets located 0.5 cm from the tube, the minimum frequency was 90 kHz. As the laser tube warmed up after turn on, the beat signal frequency cycled through its minimum as the laser line moved under the gain curve. After the tube had completely warmed up, it was possible to use a crude manual stabilization scheme to keep the laser oscillating at or very near line center. This was done by minimizing the beat frequency through either cooling the laser tube with a fan or heating it with a hot soldering iron. Although this technique was easy to implement for testing purposes, it is not suitable for automatic operation. A different technique, one which uses a PZT, was designed to perform this function.

The selection of the PZT for use in tuning the reference laser resonator was governed primarily by the fact that a high voltage operational amplifier was not available. The only amplifier that was available was a Lasermetrics Model AF-3 Audio Amplifier, which is capable of applying a signal of approximately 200 v to a capacitive load. With this 200 v limit, the specifications for the PZT were determined. The primary requirement was that the PZT should be capable of tuning the cavity over the width of the Doppler broadened gain curve (~1 GHz) in response to the 200 v. The change in resonator length required to cause this change in frequency was calculated using the equation for the resonant condition of the cavity:

$$f = \frac{cq}{2L} \tag{27}$$

where f is the resonant frequency, c is the speed of light, q is the mode number, and L is the cavity length. The derivative of Eq (27) gives the relationship between a change in cavity length (dL) and a change in the resonant frequency (df):

$$df = - \frac{cq}{2L^2} dL \tag{28}$$

or

$$|dL| = \frac{2L^2 df}{cq} \tag{29}$$

For the reference laser operating at 632.8 nm, with L = 27.48 cm, Eq (27) gives $q = 8.677 \times 10^5$. If this and the other appropriate values are substituted into Eq (29), dL is calculated to be 0.58 μm. From Ref 21 it was determined that the only PZT that could be obtained in a reasonable time was the thin disk type. For this type of PZT, the change in disk thickness occurs parallel to the applied electric field:

$$\Delta_{th} = d_{33} \cdot V \tag{30}$$

where Δ_{th} is the change in the disk thickness, d_{33} is the piezoelectric constant for this disk material (Vernitron part number 16 050-5H, $d_{33} = 590 \times 10^{-12}$ m/v), and V is the applied voltage. For ' = 200 v, Δ_{th} is only 0.118 μm. Thus, to achieve the 0.58 μm required ΔL, a stack of these disks driven in parallel is required. Eight of the disks would provide a Δ_{th} of 0.708 μm for the full 200 v from the amplifier, or these same 8 disks would provide the required Δ_{th}

of 0.58 μm with only 123 v across them.

A stack of eight of these PZT's, constructed using conducting glue and thin brass electrodes, was mounted on the laser tube using epoxy glue. The initial attempts to tune the laser with the Lasermetrics amplifier driving the PZT failed to produce any significant amount of tube stretching. This could have been caused by several problems: (1) the PZT stack may have excessively loaded down the amplifier, (2) the method of mounting the stack to the laser tube may have been faulty, or (3) a combination of the first two. There was not sufficient time to resolve this problem and to still complete other major portions of the wavemeter; therefore, no additional attempts were made to complete the stabilization subsystem.

V. Subsystem Evaluation

In this chapter, the actual performance of the different subsystems is compared to the required performance specified in Chapter III. Also, any problems that have been observed are noted. The final section of this chapter presents an estimate of the overall accuracy that could be attained with this wavemeter based on its observed performance. This estimate is given in lieu of an actual characterization based on measurements of accurately known wavelengths since the wavemeter is not yet operational.

Actual Performance

The actual performance of the wavemeter subsystems was evaluated by testing them under simulated operating conditions. The following sections discuss the current status of each of these subsystems.

Reflector Drive Subsystem. This subsystem provides the required smooth translation for the moving corner cubes. The detected fringe signals show no apparent modulation related to irregularities in the motion of the air bearing. As expected, the speed of the air bearing is slightly different in each direction of travel. The air bearing speed can be determined from the observed fringe rate and the wavelength of the detected beam (speed = fringe rate $\cdot$ λ). As the air bearing leaves the solenoid end of the V-rail, its speed is 16.6 cm/sec (= 1.05 MHz $\times$ 632.8 nm/4; the division by 4 is due to the two folds in the variable-length beam path). As

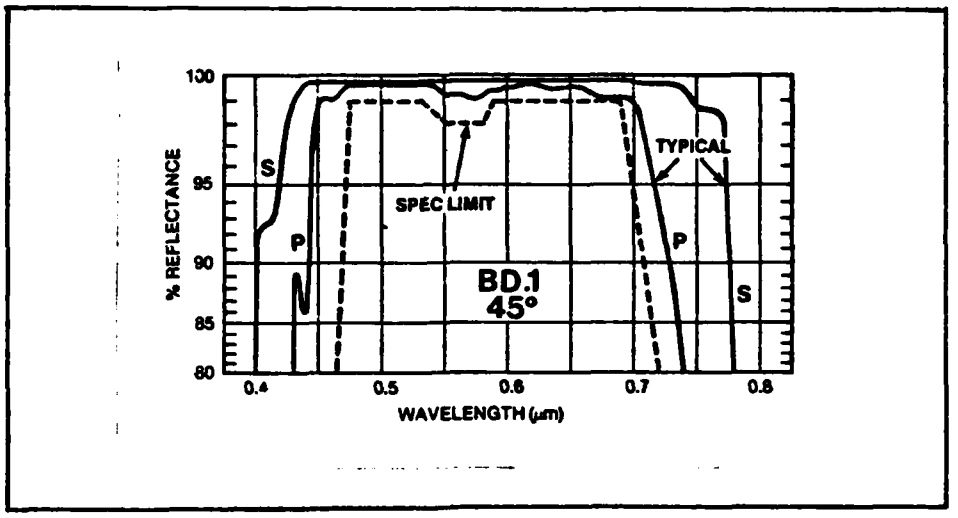

Figure 11. Mirror Reflectance vs Wavelength, NRC BD.1 Dielectric Coating (Ref 22:108)

the air bearing approaches the solenoid, its speed is 14.4 cm/sec (= 0.909 MHz × 632.8 nm/4). Since the PLL multiplier in the electronics subsystem can track the fringe rate over this much change, the speed difference presents no problem to wavemeter operation.

Beam Path Subsystem. The dielectric coating on the mirrors used in the beam path cut off at ~450 nm for the P polarization (Figure 11). This combined with the decreased sensitivity of the detector (see spectral response curve in Appendix B) may prevent proper operation of the wavemeter below 450 nm for signals with P (in this case, horizontal) polarization. However, without further testing it is not possible to conclude that operation to 400 nm cannot be achieved.

The requirement that both the reference and the unknown beams travel the same path was only verified by visual

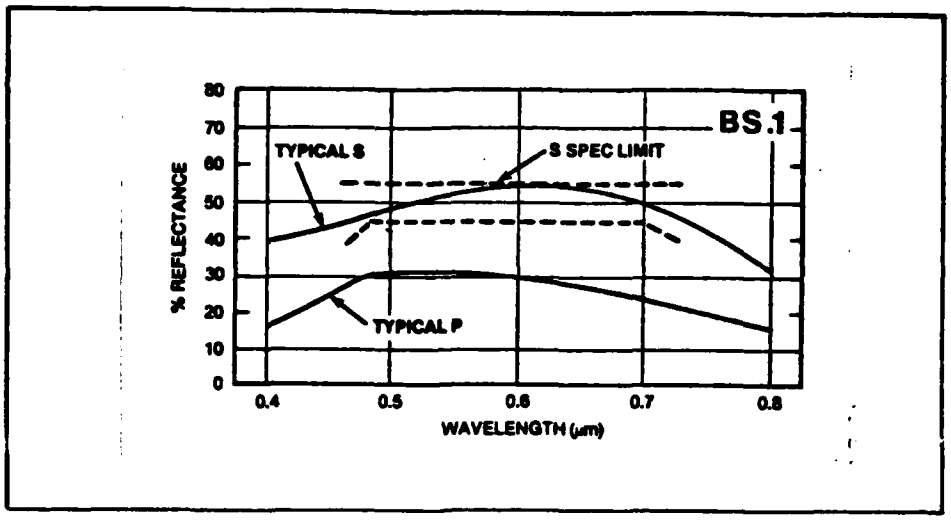

Figure 12. Beam Splitter Reflectance vs Wavelength, NRC BS.1 Dielectric Coating (Ref 22:112)

inspection. Each beam, after traveling through the optical system, falls on the output mirror of the other laser. Although this easily confirms proper alignment, it also causes a problem. Some of the energy (~2%) striking the output mirror of the other laser is reflected back through the optical system into the laser that originally radiated it. This feedback causes the laser oscillation to be unstable. A linear polarizer in front of each laser, with the transmission axis of one orthogonal to that of the other, will prevent this feedback. The orientation of these polarizers must be chosen carefully though. This is due to a characteristic of the beam splitters used in the optical path. As shown in Figure 12, the reflectance for the P polarization is less than the desired 50%. If the P polarization is selected by the polarizer, the intensities of the beams traversing the stationary and the moving paths will be much different. For the case

of the unknown beam, the moving path beam will contain ~49% of the original beam energy when it reaches the detector, while the stationary path beam will only contain ~9%. This large difference would adversely affect the fringe visibility as indicated in Chapter III.

One way the two lasers can be isolated while they both are allowed to operate with S polarization is to replace the two crossed polarizers with a single combination of a linear polarizer and a quarter-wave plate at the output of the reference laser. This combination will keep retroreflections from causing instabilities. This combination also removes one of the Zeeman components from the output of the reference laser. This prevents the beat signal from the two Zeeman components from appearing in the output of the fringe detector.

Another factor which could affect the relative intensities of the beams traveling the stationary and the moving paths is the difference in overall path lengths. As the moving reflector travels the length of the V-rail, the difference in the length of the stationary path from the moving path varies from -93 cm to +63 cm. The detected fringe signal shows no apparent change in fringe visibility related to the difference in overall path lengths.

A problem that was noted while the beam path subsystem was being aligned, was an apparent amplitude modulation of the detected fringe signal. The peaks and troughs of the modulation were related to the position of the moving reflector. The source of the problem was determined to be the

multimode output of the unknown laser used during testing. The laser was operating on two linearly polarized modes, each of which was generating a fringe pattern as the reflector moved. Due to the frequency difference between the two modes, the two fringe patterns would alternately constructively and destructively interfer which caused the amplitude peaks and troughs in the detected signal. When one of the modes is filtered out or when the unknown laser oscillates on a single mode, this amplitude modulation is not a problem.

Electronics Subsystem. The major problem with the electronics subsystem in its present form is that the fringe signals from the detectors (~2 mv p-p) have not yet been successfully amplified to the voltage levels required by the counting circuits. An amplifier circuit using a Motorola MC1590G amplifier was constructed, but its output failed to meet the voltage level requirements. Until the fringe signal is properly conditioned, the wavemeter will not function. Even though the wavemeter was not functioning, it was possible to evaluate the operation of some of the electronic circuits.

The reference and unknown fringe counting channels and the microcomputer were tested together. A simulated fringe signal (1 MHz sine wave) from a Wavetek Model 148 Waveform Generator was applied simultaneously to both counting channels. The microcomputer was programmed to display the reference count at the end of each counting sequence. This arrangement tested the counting and display circuits, and

the input/output capability of the microcomputer. Perfect operation of the counters would have resulted in the unknown count being exactly 20 times the reference count (2^{21}). The actual unknown count varied slightly from this. The standard deviation of the count was measured to be 5.45 counts over 175 counting cycles. This would limit the system accuracy to 1.3 parts in 10^7. A modification in the way the counting cycle is started removed this error. This change is included in the schematic (Figure 15).

The microcomputer section worked exactly as expected. Input, output, and control of the counters was accomplished under program direction. Also, the microcomputer's link to an external computer was tested. The count of the simulated reference fringes described previously was sent over an RS232 serial data link to the laboratory LSI-11 computer, where it was successfully read and stored. The assembly language routines used in the microcomputer program to calculate the wavelength were tested for accuracy by use of an interactive computer terminal. The fringe count ratios and control line inputs were entered from a keyboard rather than from the wavemeter hardware. The wavelengths that the assembly language program calculated agree with those calculated using a high level language (Pascal) on a DEC PDP-11/60. Table I shows the actual values used in this comparison. It should be noted that the program used in the wavemeter uses the ninth significant digit to round the eight most significant digits.

TABLE I

Comparison of Calculated Wavelengths

Count Ratio	Wavemeter Program		PDP 11/60 Program	
	$\lambda_{air(nm)}$	$\lambda_{vac(nm)}$	$\lambda_{air(nm)}$	$\lambda_{vac(nm)}$
1.234041	512.78685	512.92973	512.7868523	512.9297333
1.531502	413.18914	413.30570	413.1891444	413.3056945
0.946055	668.88289	669.06756	668.8828874	669.0675642

Reference Laser Subsystem. As indicated in Chapter IV, the reference laser subsystem was not completed due to problems with the PZT. This seriously impacts the achievable accuracy of the wavemeter since the reference laser wavelength is now known only approximately. This is due to the fact that the oscillation mode of the reference laser could be located anywhere under the Doppler broadened gain curve. Thus, the accuracy is limited to $\Delta f/f$ where Δf is the width of the Doppler broadened gain curve and f is the laser oscillation frequency (c/λ). With the reference laser used in this system, the maximum achievable accuracy is $(1.08 \times 10^{9})/(4.74 \times 10^{14}) = 2.3 \times 10^{-6}$. This is less than half as accurate as is required in the design specification and an order of magnitude less than the desired accuracy.

Accuracy Estimate

Out of all of the problems noted in this chapter, the only one which directly affects the accuracy of the wavemeter is the lack of a stable frequency reference laser. Another problem, the low voltage level of the fringe detection circuit, prevents any operation of the wavemeter at all; however, even if that problem was overcome, the lack of stabilization

would still limit the wavemeter accuracy to 2.3×10^{-6}, as calculated in the preceeding section. When the frequency of the reference laser is stabilized, the overall system accuracy should meet the design goal.

VI. Conclusions and Recommendations

In this thesis project, a wavemeter has been designed and partially fabricated. The original intent was to complete the design and fabrication and then to characterize the performance of the system. Problems with some of the subsystems prevented completion of the wavemeter and thus characterization was not possible. After the extent of the problems was examined, it was concluded that there is no basic limitation with those portions of the wavemeter that were completed and that with additional work the wavemeter could be completed and meet the design specifications.

Based on an evaluation of the cause of the problems which prevented completion of this project, the following recommendations are presented:

1. A high voltage operational amplifier should be obtained for driving the PZT used to stabilize the frequency of the reference laser.
2. The electronic circuit used to stabilize the reference laser should be completed.
3. An ac coupled amplifier capable of providing a voltage gain of ~800 should be constructed for use in the fringe detection circuit.

Bibliography

1. Hecht, E. and A. Zajac. Optics. Boston: Addison-Wesley Publishing Co, 1979.

2. Snyder, J.J. "Laser Wavelength Meters," Laser Focus, 18: 55-61 (May 1982).

3. Juncar, P. and J. Pinard. "A New Method for Frequency Calibration and Control of a Laser," Optical Communications, 14: 438-441 (1975).

4. Byer, R.L., et al. "A Wavelength Meter" in Laser Spectroscopy III, edited by J.L. Hall and J.L. Carlsten, New York: Springer-Verlag, 1977.

5. Pole, R. and R. Salimbeni. "Compact High-Accuracy Wavemeter," Optics Letters, 5 (2): 39-41 (February 1980).

6. Hall, J.L. and S.A. Lee. "Interferometric Real-Time Display of CW Dye Laser Wavelength with Sub-Doppler Accuracy," Applied Physics Letters, 29 (6): 367-369 (15 September 1976).

7. Demtröder, W., et al. "An Improved Wavemeter for CW Lasers," Journal of the Optical Society of America, 68 (11): 1611-1613 (November 1978).

8. Ciarcia, A. Build Your Own Z80 Computer - Design Guidelines and Application Notes. New Hampshire: McGraw-Hill, 1981.

9. Klein, M.L. Optics. New York: John Wiley & Sons, Inc., 1970.

10. Jenkins, F.A. and H.E. White. Fundamentals of Optics (Third Edition). New York: McGraw-Hill Book Company, 1957.

11. Wood, R.W. Physical Optics (Third Edition). New York: The Macmillan Co., 1934.

12. Yariv, A. Introduction to Optical Electronics. New York: Holt, Rinehart, and Winston, 1976.

13. Fork, R.L. and W.J. Tomlinson. "Properties of Gaseous Optical Masers in Weak Axial Magnetic Fields," Physical Review, 164 (2): 466-483 (10 December 1967).

14. Baer, T., et al. "Frequency Stabilization of a 0.633-μm He-Ne Longitudinal Zeeman Laser," Applied Optics, 19 (18): 3173-3178 (15 September 1980).

15. Baird, D.C. Experimentation: An Introduction to Measurement Theory and Experimental Design. Englewood Cliffs: Prentice-Hall, Inc., 1962.

16. Bozman, W.R., et al. Table of Wavenumbers, Vol 1. National Bureau of Standards Monograph 3, Washington, D.C.: US Government Printing Office, 1960.

17. Drullinger, R., Physicist, Personal Interview, Time and Frequency Division, National Bureau of Standards, Boulder, CO (1 July 1982).

18. Mano, M.M. Digital Logic and Computer Design. Englewood Cliffs: Prentice-Hall, Inc., 1979.

19. Rogers, D. and M. Ross. Z-80 Microcomputer, Unpublished Senior Design Project (EE 4.90), School of Engineering, Air Force Institute of Technology, Dayton, Ohio, March 1982.

20. Wadsworth, N. Z80 Software Gourmet Guide & Cookbook. Elmwood, CT: Scelbi Publications, 1979.

21. Lee, P. Customer Service (Telephone 216-232-8600), Private Communication, Vernitron, Bedford, OH (3 June 1982).

22. Newport Research Corporation, Product Catalog, 1981.

23. EG&G ElectroOptics, Data Sheet D3013B-1. Salem, MA (1979).

APPENDIX A

Air Bearing Construction

This Appendix contains a drawing of the air bearing that was constructed for use in this project. The actual fabrication of the piece was done at the AFIT Model Fabrication Division by Mr. Russell Murray.

Although not shown in Figure 13, the air bearing was fabricated from two brass blocks. This was required since a large enough single piece was not available. The faces of the V were milled into the two pieces before they were glued and bolted together. The air chambers that run the length of the device were bored from one end and do not go entirely through the block. Before the ends of these air chambers were plugged, the feed tube holes were drilled in from the sides and the four 0.020 inch exit holes were drilled in from the faces of the V. All drilling debris was carefully removed prior to plugging the ends of the air chambers.

Dr. Drullinger, of the National Bureau of Standards (Ref 17), provided the following tips concerning construction of an air bearing in the inverted configuration:

1. The exit holes should have smaller diameters than any of the other passages in the air system.
2. The exit holes should be located halfway up the sides of the V.
3. Only two holes per face are required and they should be separated by about two thirds the length of the air bearing.

4. The angle between the air bearing faces should be 90°.

5. The surfaces of the air bearing faces and the V-rail should be as smooth as possible.

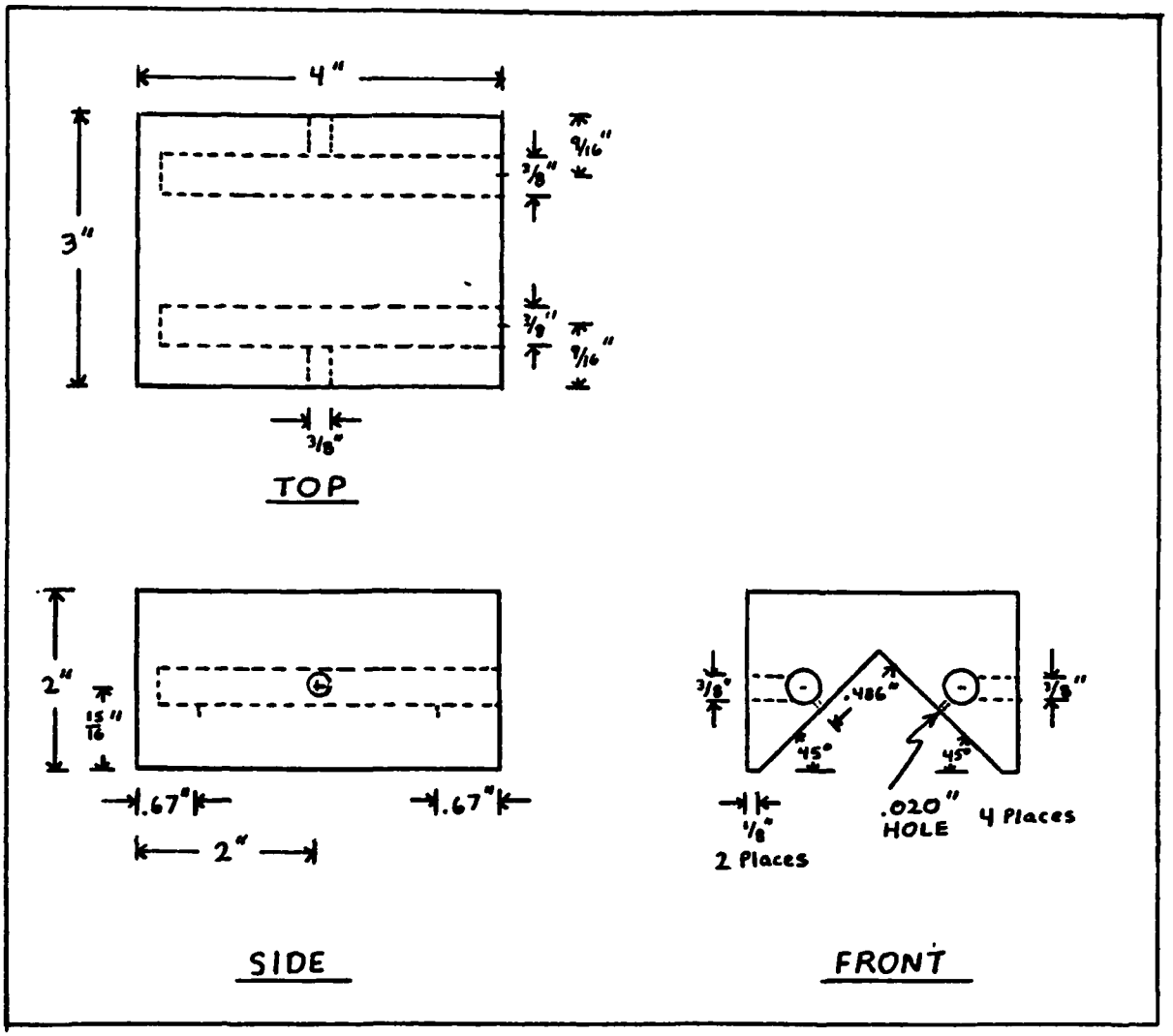

Figure 13. Details of Air Bearing Construction

APPENDIX B

Detector Data

The FND-100 is a silicon photodiode which is used for fringe detection. Table II contains information on its performance characteristics and Figure 14 shows its spectral response.

TABLE II

FND-100 Performance

Characteristic	Typical Value
Active Area	5.1 mm^2
Bandwidth	350 MHz
Responsivity	0.62 A/w @ 900 nm
Rise Time (10-90%)	<1 nsec @ 50 Ω
Operating Voltage	90 v
Breakdown Voltage	>125 v
Capacitance	8.5 pf
Series Resistance	35 Ω

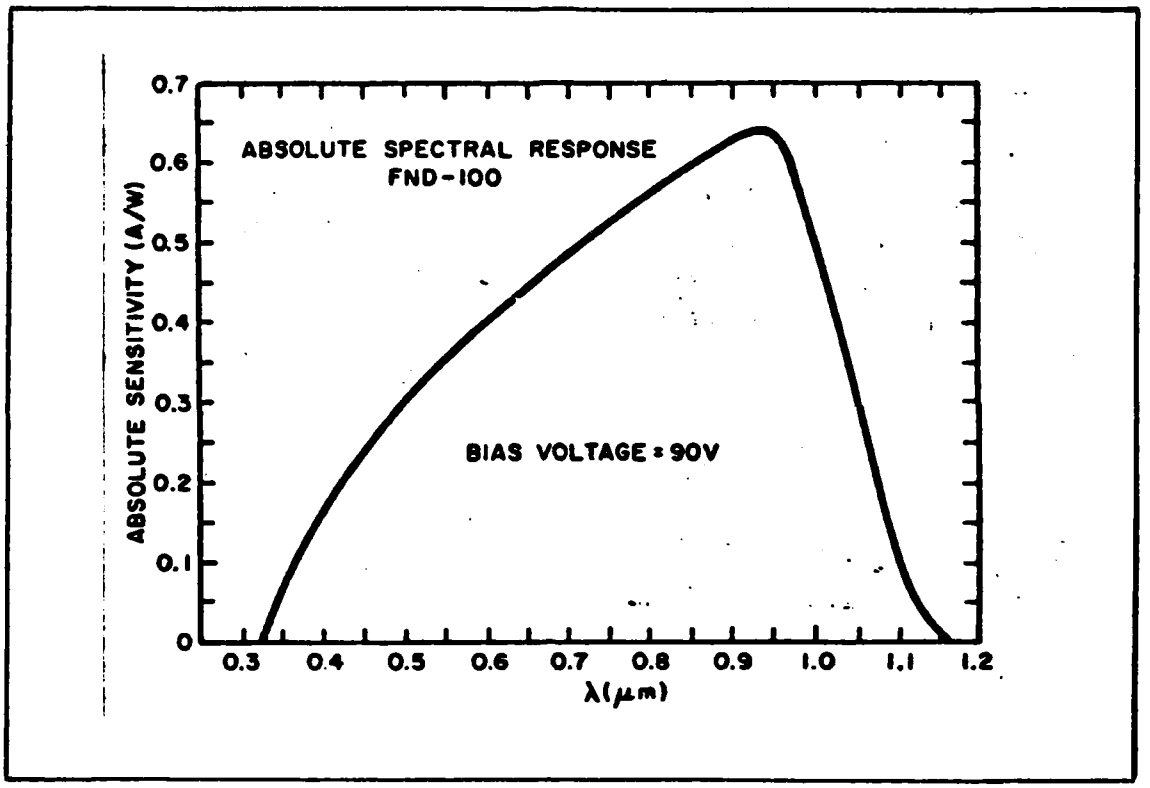

Figure 14. FND-100 Spectral Response (Ref 23).

APPENDIX C

Schematic Diagrams

This Appendix contains schematic diagrams of electronic circuits used in the wavemeter. A description of each is provided.

The fringe counting circuit of Figure 15 works as follows: The OPTICAL SWITCH input gates the fringe signals into the counter channels. The 74122 retriggerable one-shot is used to activate both channels when the first reference pulse is detected. When the three 54393 counters have counted 2^{21} reference fringes, the 74S10 turns off the inputs to both counter channels and triggers the 74121 one-shot which latches the unknown fringe count held by the four 74LS393 counters into the four 74LS373 tri-state latches. The NE564 PLL multiplies the unknown fringe count by 20. It does this by dividing the VCO signal by 20 (using the 5490 and 7490 counters) before comparing it with the input fringe signal. The VCO output is then counted by the counter channel. The four OUTPUT ENABLE lines are sequentially strobed by the microcomputer to read out the unknown fringe count. The CLEAR COUNT input from the microcomputer clears the counters by momentarily putting a logic one to the reset pins on the counters. The connections between the counters and the latches are shown only for one of the counter and latch chip pairs. The remaining three pairs are connected exactly like the first pair. Also, the connections from the

latches to the microcomputer data bus are only shown once. The connections for the remaining latches are identical to the one shown.

The reversible counter circuit of Figure 16 works as follows: The 2.0000 MHz signal from the crystal is divided by the 74393, 7490, 7493, and 7408 integrated circuits to provide an ~11 Hz square wave which is used to alternate the four 74193 counters between counting up and counting down at the beat frequency. At the end of each up/down count cycle, the 74121 one-shot triggers and, while inhibiting input to the counters, latches the current residual count into the 74373 tri-state latches.

The beat frequency detection circuit of Figure 17 provides an amplified signal which can drive a switching transistor to provide a TTL compatible signal to the reversible counter circuit.

The optical switch circuit of Figure 18 works as follows: While light from the 5 v bulbs at the ends of the air rail is incident on the MRD14B photo-Darlingtons, the 2N2222 transistors are saturated, providing a logic one to the 74121 one-shot. When the beam to either photo-Darlington is blocked, the input to the one-shot goes low, causing the output to go low for a time determined by the setting of the potentiometer. The duration of this low level pulse is adjusted to allow enough time for the air bearing to reverse direction and to unblock the beam before the output goes high again.

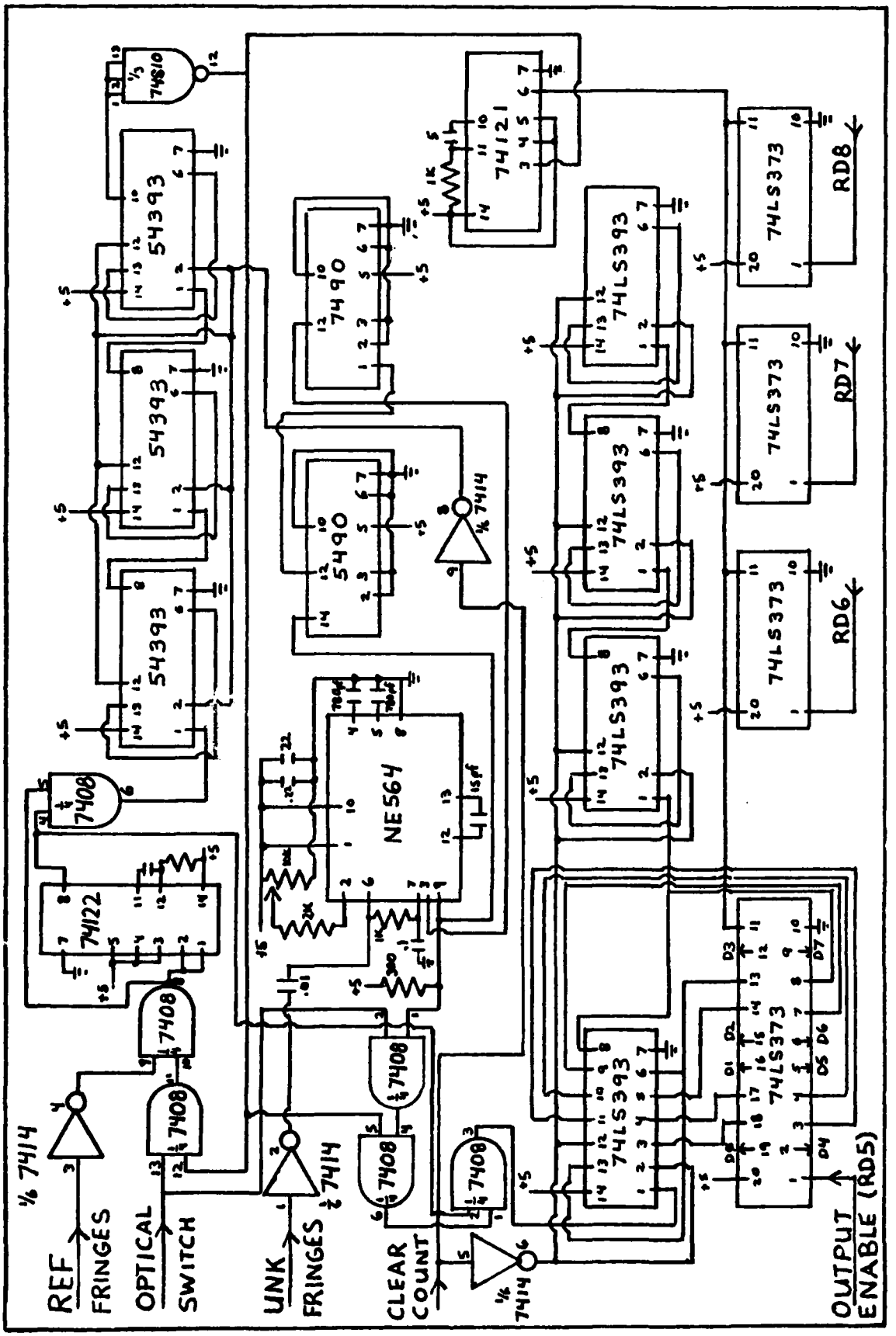

Figure 15. Fringe Counting Circuit Schematic Diagram

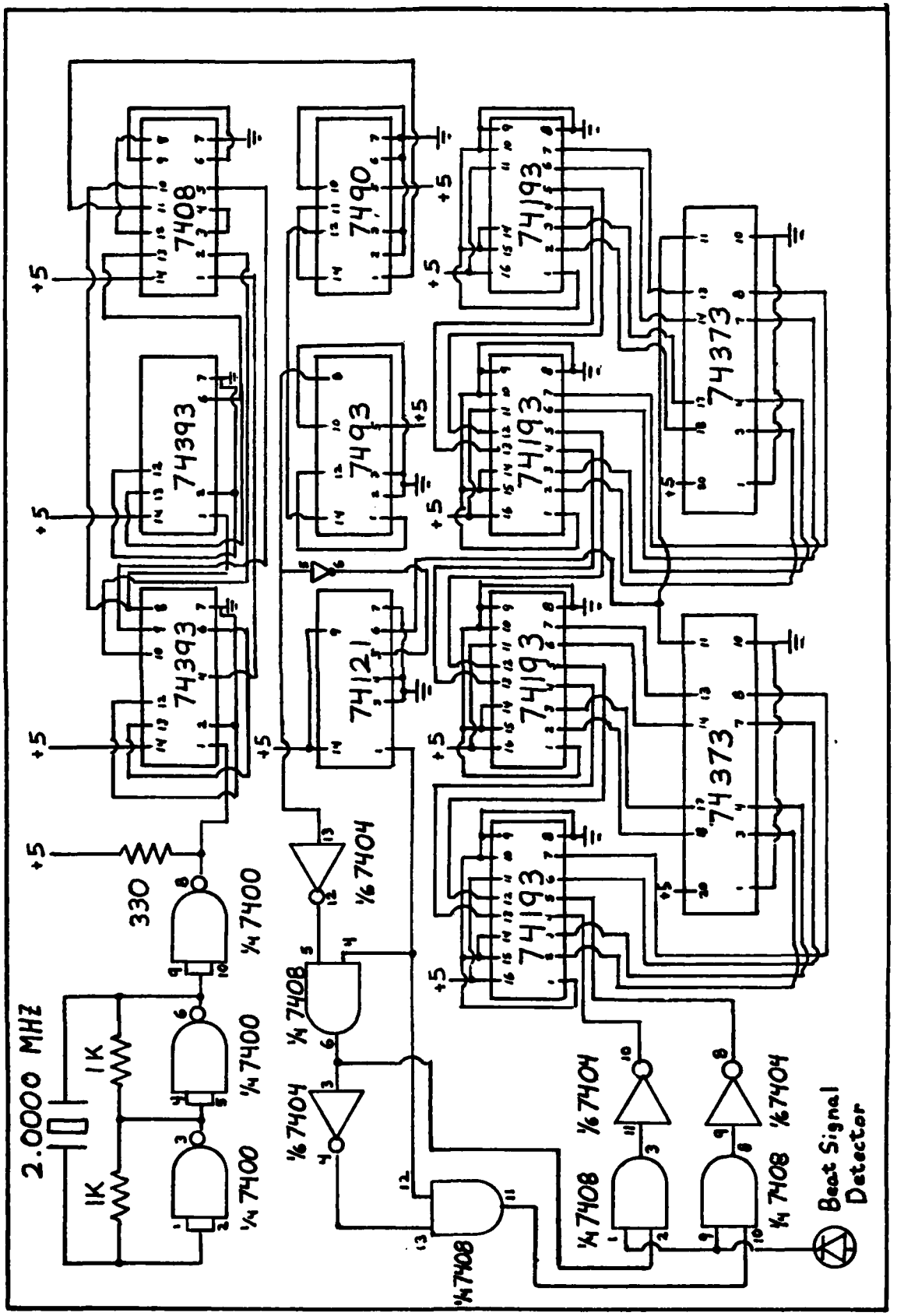

Figure 16. Reversible Counter Schematic Diagram

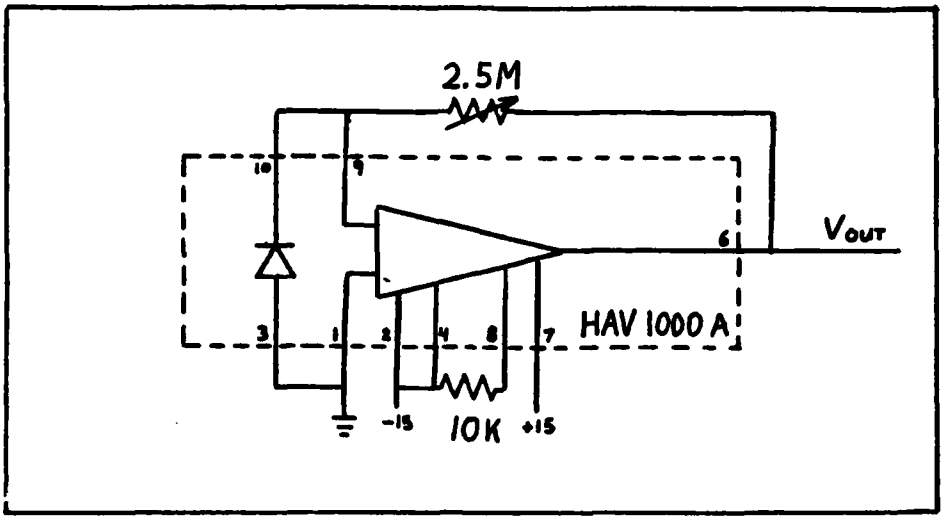

Figure 17. Beat Frequency Detection Circuit Schematic Diagram

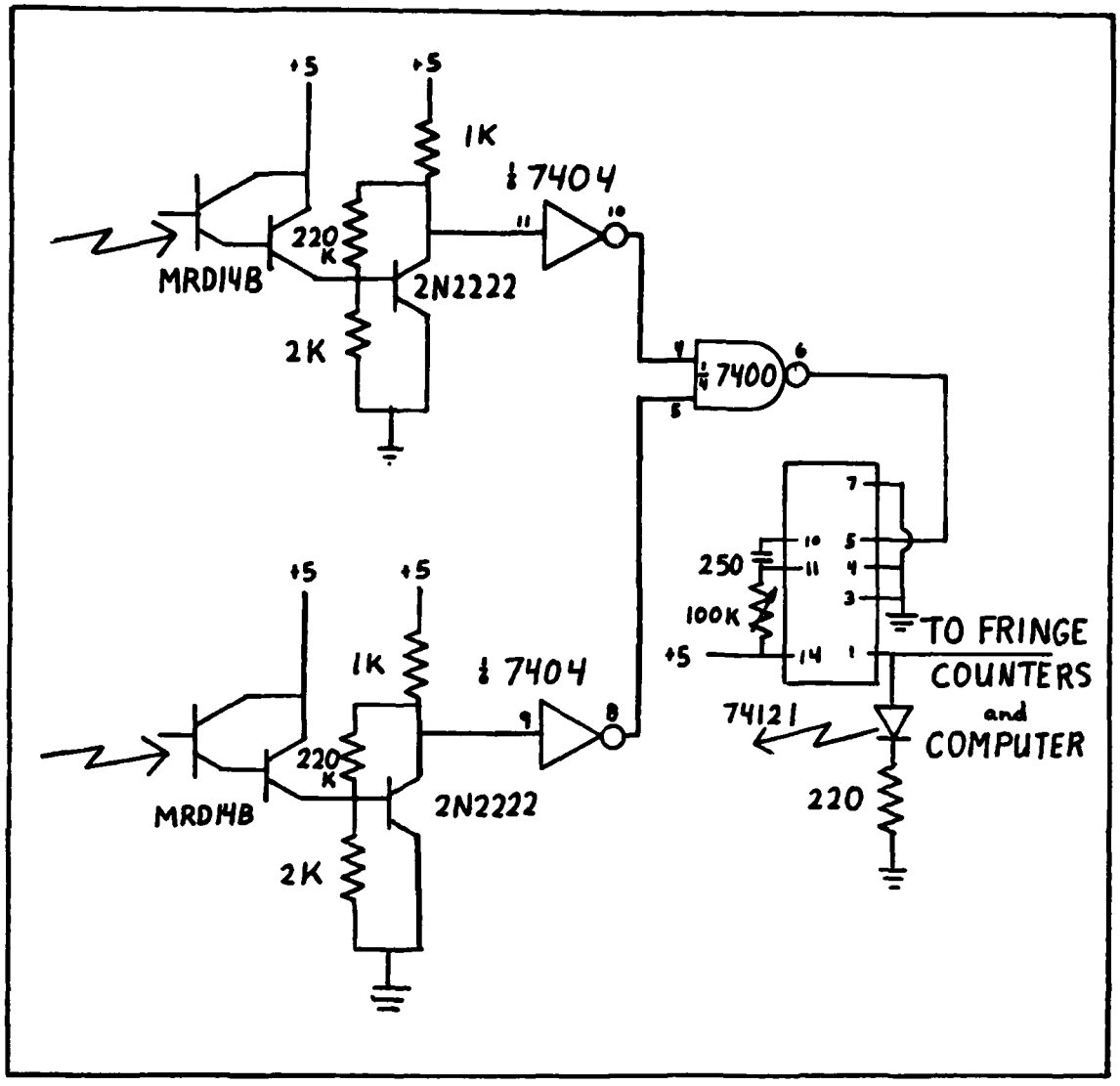

Figure 18. Optical Switch Schematic Diagram

APPENDIX D

Program Flow Charts

This Appendix contains flow charts for the primary routines used in the wavemeter program. Symbols which have not already been defined are defined below:

LREFA: λ_r in air

LREFV: λ_r in vacuum

LTEMP: dummy variable - holds old value of LUNKV

LUNKA: λ_u in air

LUNKV: λ_u in vacuum

NREF: index of refraction of air at LREFA

NUNK: index of refraction of air at LUNKA

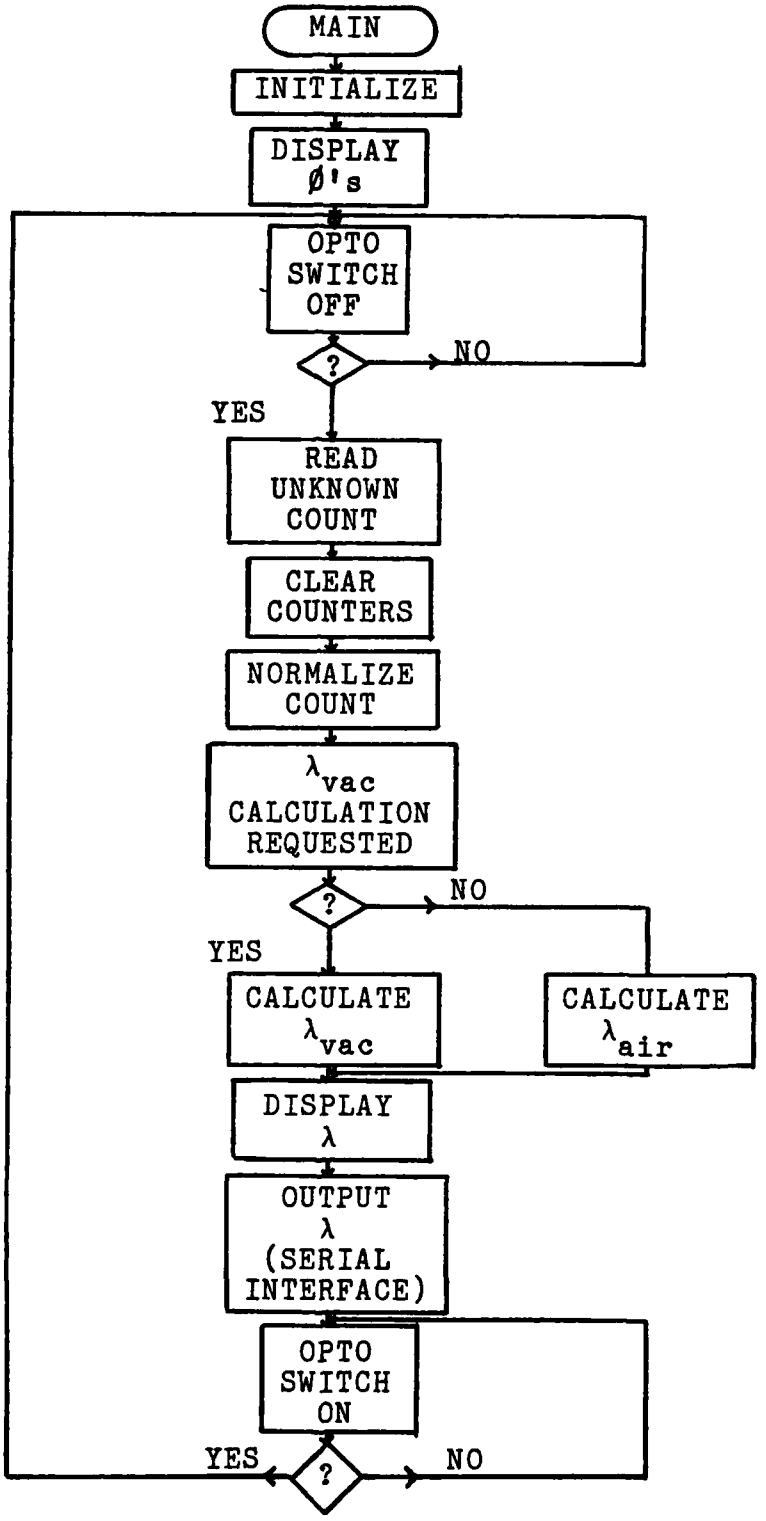

Figure 19. Microcomputer Main Program Flow Chart

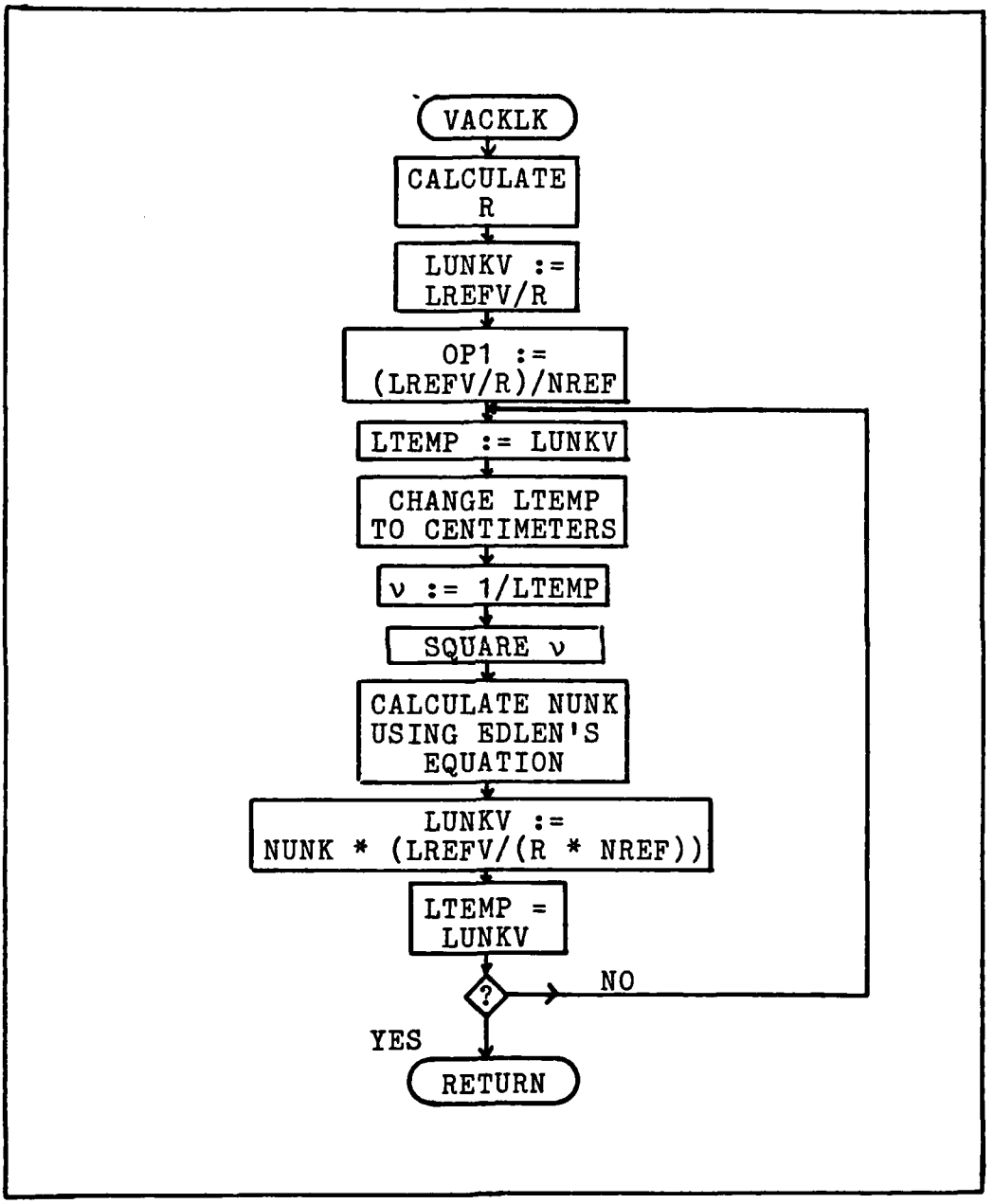

Figure 20. Vacuum Wavelength Calculation Subroutine Flow Chart

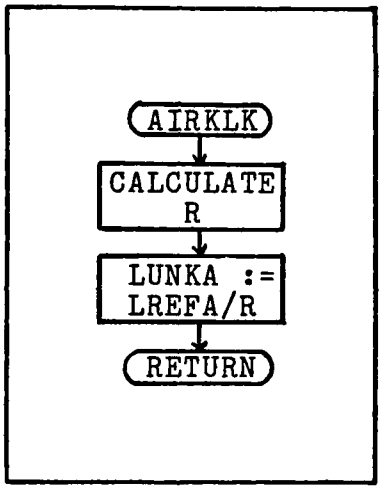

Figure 21. Air Wavelength Calculation Subroutine Flow Chart

Vita

Harry W. Ladewig, son of CMSgt (Ret.) Earl and Freda Ladewig, was born on 15 October, 1950 in Denver, Colorado. He graduated from high school in Athens, Greece in 1968 and enrolled at Colorado State University, Ft. Collins, Colorado. While there, he received a scholarship from the Air Force ROTC and majored in Electrical Engineering. In June 1973, he was awarded the Degree of Bachelor of Science with Distinction. He was also selected as a Distinguished Military Graduate of the ROTC program and was commissioned in the USAF. His first assignment was with the Air Force Electronic Warfare Center (AFEWC), Kelly AFB, Texas where he was assigned as an Electronic Warfare Development Engineer. From 1978 to 1981, he represented the AFEWC as an Electronic Warfare Liaison Officer at Headquarters, European Command, Stuttgart-Vaihingen, Germany. In 1981, he entered the School of Engineering, Air Force Institute of Technology.

UNCLASSIFIED

SECURITY CLASSIFICATION OF THIS PAGE *(When Data Entered)*

REPORT DOCUMENTATION PAGE

READ INSTRUCTIONS BEFORE COMPLETING FORM

1. REPORT NUMBER: AFIT/GEO/PH/82D-7	2. GOVT ACCESSION NO.: AD-A124 759
3. RECIPIENT'S CATALOG NUMBER:	
4. TITLE *(and Subtitle)*: DESIGN AND DEVELOPMENT OF A LASER WAVEMETER	5. TYPE OF REPORT & PERIOD COVERED: MS Thesis
	6. PERFORMING ORG. REPORT NUMBER:
7. AUTHOR(s): Harry W. Ladewig	8. CONTRACT OR GRANT NUMBER(s):
9. PERFORMING ORGANIZATION NAME AND ADDRESS: Air Force Institute of Technology (AFIT-EN) Wright-Patterson AFB, Ohio 45433	10. PROGRAM ELEMENT, PROJECT, TASK AREA & WORK UNIT NUMBERS:
11. CONTROLLING OFFICE NAME AND ADDRESS:	12. REPORT DATE: December, 1982
	13. NUMBER OF PAGES: 82
14. MONITORING AGENCY NAME & ADDRESS *(if different from Controlling Office)*:	15. SECURITY CLASS. *(of this report)*: Unclassified
	15a. DECLASSIFICATION/DOWNGRADING SCHEDULE:

16. DISTRIBUTION STATEMENT *(of this Report)*

Approved for public release; distribution unlimited

17. DISTRIBUTION STATEMENT *(of the abstract entered in Block 20, if different from Report)*

18. SUPPLEMENTARY NOTES

Approved for public release: IAW AFR 190-17

LYNN E. WOLAVER
Dean for Research and Professional Development
Air Force Institute of Technology (AU)
Wright-Patterson AFB OH 45433

16 JAN 83

19. KEY WORDS *(Continue on reverse side if necessary and identify by block number)*

Wavemeter
Laser Wavemeter
Wavelength Measurement
Moving Arm Interferometer
Laser Frequency Stabilization
Zeeman Frequency Stabilization
Michelson Interferometer

20. ABSTRACT *(Continue on reverse side if necessary and identify by block number)*

The purpose of this thesis project is to design and fabricate a wavemeter suitable for measuring the wavelength of visible, continuous wave laser emissions. After a review of the literature, a moving-arm Michelson interferometer was selected as the basis for the wavemeter. A twice folded path is used in the moving arm and electronic fringe rate multiplication is used in the counting circuit to improve system accuracy without increasing its overall

DD FORM 1 JAN 73 1473 EDITION OF 1 NOV 65 IS OBSOLETE

UNCLASSIFIED

SECURITY CLASSIFICATION OF THIS PAGE *(When Data Entered)*

size. A Z80 based microcomputer is incorporated in the system for control and calculation purposes. Its use allows corrections to be made for the dispersion of air when the vacuum wavelength is calculated. Constraints on the wavemeter subsystems are derived from the basic design specifications. A description of the fringe counting circuits, and the wavelength calculation algorithms, is presented. The portions of the wavemeter that were constructed are evaluated in regard to how well they meet the design specifications. Problems in stabilizing the frequency of the reference laser and amplifying the detected fringe signals prevented completion of the wavemeter. Recommendations are made concerning additional work that must be done to complete its fabrication.

END

FILMED

3-83

DTIC